

1 **FOXO1 represses *Sprouty2* and *Sprouty4* expression**
2 **in endothelial cells to promote arterial specification and vascular remodeling**
3 **in the mouse yolk sac**

4
5 Nanbing Li-Villarreal*, Rebecca Lee Yean Wong*, Monica D. Garcia*, Ryan S. Udan, Ross A.
6 Poché, Tara L. Rasmussen, Alexander M. Rhyner, Joshua D. Wythe, and Mary E. Dickinson**

7
8 Department of Molecular Physiology & Biophysics, Baylor College of Medicine. One Baylor
9 Plaza, Houston, Texas 77030.

10
11 * Authors who contributed equally to the work

12 ** Correspondence: mdickins@bcm.edu

13

14 **ABSTRACT**

15 The establishment of a functional circulatory system is required for post-implantation
16 development during murine embryogenesis. Previous studies in loss of function mouse models
17 have shown that FOXO1, a Forkhead family transcription factor, is required for yolk sac vascular
18 remodeling and survival beyond embryonic day (E) 11. Here, we demonstrate that loss of
19 *FoxO1* in E8.25 endothelial cells results in increased *Sprouty2* and *Sprouty4* transcripts,
20 reduced expression of arterial genes, and decreased *Flk1/Vegfr2* mRNA levels without affecting
21 overall endothelial cell identity, survival, or proliferation. Using a *Dll4-BAC-nlacZ* reporter line,
22 we found that one of the earliest expressed arterial genes, *Delta like 4 (Dll4)*, is significantly
23 reduced in the yolk sac of *FoxO1* mutants without being substantially affected in the embryo
24 proper. We show that in the yolk sac, FOXO1 not only binds directly to a subset of previously
25 identified *Sprouty2* gene regulatory elements (GREs), as well as newly identified, evolutionarily
26 conserved *Sprouty4* GREs, but can also repress their expression. Additionally, over expression
27 of *Sprouty4* in transient transgenic embryos largely recapitulates reduced expression of arterial
28 genes seen in endothelial *FoxO1* mutant mouse embryos. Together, these data reveal a novel
29 role for FOXO1 as a key early transcriptional repressor controlling both pre-flow arterial
30 specification and subsequent vessel remodeling within the murine yolk sac.

31

32

33 INTRODUCTION

34 During early development the mammalian embryo requires a functional circulatory
35 system to distribute oxygen, nutrients, and hormones. The mammalian heart is the first organ to
36 form and function within this early embryo, along with the first arteries and veins that arise de
37 novo via vasculogenesis (Fish and Wythe, 2015, Risau, 1994, Risau and Flamme, 1995, Chong
38 et al., 2011). Primitive erythrocytes form in the blood islands of the extra-embryonic yolk sac
39 (YS), and are drawn into circulation as the heart begins to beat around embryonic day (E) 8 in
40 the mouse embryo (Lucitti et al., 2007, Palis, 2014, Ji et al., 2003). A complete circulatory loop
41 between the embryo and the extra-embryonic YS is evident shortly after the onset of cardiac
42 contractions, with blood flowing through the dorsal aorta to the vitelline (omphalomesenteric)
43 artery (VA), through the YS capillary plexus, and back through the vitelline (omphalomesenteric)
44 vein (VV) to the sinus venosus of the heart. Circulation through the YS is the main circulatory
45 loop until the chorion-allantoic placenta connections develop later around E9.

46 A key finding several years ago showed that arterial-venous (AV) identity is established
47 prior to the onset of blood flow in the early mouse embryo (Herzog et al., 2005, Chong et al.,
48 2011, Aitsebaomo et al., 2008, Wang et al., 1998, Adams et al., 1999). Others have since
49 shown that some aspects of AV identity are plastic, as they can be influenced by changes in
50 blood flow and hemodynamics (le Noble et al., 2004, le Noble et al., 2005, Wragg et al., 2014).
51 Extensive work in zebrafish has shown that AV specification depends on differential responses
52 to VEGF signaling through the tyrosine kinase receptor VEGFR2/Fik1, high levels of which
53 activate the MEK/ERK kinase cascade in arterial cells and PI3K/AKT signaling in venous cells
54 (Fish and Wythe, 2015, Covassin et al., 2006, Weinstein and Lawson, 2002). In the arterial
55 endothelium, VEGFR2 signaling stimulates the Notch pathway, which in turn promotes an
56 arterial identity while simultaneously repressing a venous fate (Weinstein and Lawson, 2002,
57 Krebs et al., 2010, Lawson et al., 2001, Lawson et al., 2002, Liu et al., 2003, Shutter et al.,
58 2000, Swift and Weinstein, 2009, Siekmann and Lawson, 2007, Krebs et al., 2000, Duarte et al.,

59 2004, Lobov et al., 2007). VEGF upregulates expression of *Delta-like 4 (Dll4)*, which encodes a
60 ligand for the Notch family of transmembrane receptors. *Dll4* is the earliest Notch ligand
61 expressed in arterial cells in the early mouse embryo (Shutter et al., 2000, Mailhos et al., 2001,
62 Wythe et al., 2013, Cleaver and Krieg, 1998, Chong et al., 2011), and is essential for AV
63 patterning (Krebs et al., 2000, Gale et al., 2004, Duarte et al., 2004). Expression of *Dll4*
64 depends on the activation of ETS transcription factors, downstream of VEGF signaling (Wythe
65 et al., 2013, Fish et al., 2017) and *Dll4* mRNA expression can be increased by shear stress
66 (Masumura et al., 2009, Obi et al., 2009). However, the expression of *Dll4* and a few other
67 select arterial markers prior to, and independent of, the onset of blood flow (Chong et al., 2011,
68 Wang et al., 1998) suggests flow-independent mechanisms regulate arterial specification.
69 *Vegfr2* also upregulates expression of the main endothelial cell surface receptor for *Dll4*, *Notch1*
70 (Lawson et al., 2002). *Notch* itself is activated by blood flow and the strength of this signal
71 depends on the magnitude of shear stress (Masumura et al., 2009, Mack et al., 2017). *Notch*
72 regulates cell junctions, cell cycle arrest, and induces an arterial gene expression program via a
73 *connexin37 (Gja4)/p27^{Kip1} (Cdkn1B)* pathway (Mack et al., 2017, Su et al., 2018, Fang et al.,
74 2017). Critically, both *Vegfr2* and *Notch1* are thought to act as mechanosensors, likely linking
75 arterial specification of ECs and hemodynamic feedback via blood flow to re-enforce and solidify
76 their arterial identity (Mack et al., 2017, Tzima et al., 2005, Mack and Iruela-Arispe, 2018, Shay-
77 Salit et al., 2002).

78 Forces exerted by blood flow play a clear role in AV specification, and also influence
79 vessel morphogenesis and remodeling in the early embryo (Fang et al., 2017, Masumura et al.,
80 2009, le Noble et al., 2004, Chong et al., 2011, Hwa et al., 2017). Hemodynamic force is both
81 necessary and sufficient to remodel the high-resistance mouse YS capillary plexus into a more
82 complex hierarchical network with a large caliber VA and VV progressively leading to smaller
83 diameter vessels (Lucitti et al., 2007). Our lab has shown that murine yolk sac vessel
84 remodeling depends on both vessel fusion and EC migration (Udan et al., 2013). Interestingly,

85 live imaging studies showed distinct differences in how arterial and venous cells respond to
86 changes in hemodynamic force (Udan et al., 2013, Kondrychyn et al., 2020, Goetz et al., 2014).
87 These data suggest that pathways that control AV identity, which can be regulated by blood
88 flow, may also influence physical responses of ECs to blood flow such as migration and motility
89 that facilitate vessel remodeling.

90 Despite the knowledge that has been gained regarding the mechanisms regulating
91 arterial-venous identity and the discovery of mechanosensors that are required for ECs to sense
92 blood flow, a full understanding of these mechanistic pathways is yet to be realized. A recent
93 analysis estimates that approximately 6% of genes in the genome (~1200) may be required
94 during early cardiovascular development (E9.5-E12.5) (Dickinson et al., 2016). One such gene,
95 and the focus of this study, is *FoxO1* (*Forkhead box protein O1*). *Forkhead domain class O*
96 *transcription factors* (FOXOs) integrate different cellular signaling pathways to regulate cellular
97 homeostasis (Paik et al., 2007, Huang and Tindall, 2007, Jiramongkol and Lam, 2020). *Daf-*
98 *16/FoxO* was originally identified as a regulator of dauer formation in *C. elegans* (Albert et al.,
99 1981) and was later shown to control longevity by sensing environmental cues such as
100 hormones, nutrient availability, oxidative stress, and energy metabolism via signaling through
101 the insulin, AKT/mTor, JNK and AMPK pathways (Sun et al., 2017). Several studies have since
102 established that *FoxO1* is also required for normal embryonic development in mice.
103 Homozygous null *FoxO1* embryos display a primitive yolk sac vasculature, pericardial edema,
104 and disorganized embryonic vessels by E9.5, resulting in lethality by E11.5 (Furuyama et al.,
105 2004, Dharaneeswaran et al., 2014, Hosaka et al., 2004, Sengupta et al., 2012, Wilhelm et al.,
106 2016, Ferdous et al., 2011). Further analysis showed that loss of *FoxO1* in the endothelium, but
107 not the myocardium, phenocopied germline loss of *FoxO1* (Sengupta et al., 2012),
108 demonstrating the cell autonomous requirement for FOXO1 in the embryonic vasculature.
109 Follow-up studies have since found that FOXO1 controls a variety of different processes in
110 endothelial cells (ECs), including, but not limited to EC proliferation and metabolism (Wilhelm et

111 al., 2016), endothelial barrier function (Beard et al., 2020), sprouting angiogenesis (Kim et al.,
112 2019, Fukumoto et al., 2018, Dang et al., 2017), autophagy (Zhang et al., 2019), EC growth
113 (Riddell et al., 2018, Rudnicki et al., 2018) and migration (Niimi et al., 2017). Despite these
114 studies, the exact function that FOXO1 plays in the early vasculature remains elusive. Given
115 that FOXO1 activity can be modulated in response to fluid shear stress (Chlench et al., 2007,
116 Dixit et al., 2008), combined with our studies showing that hemodynamic force is necessary and
117 sufficient for early vascular remodeling (Lucitti et al., 2007, Udan et al., 2013), and the growing
118 evidence for FOXO1 in cell migration and sprouting angiogenesis (Fosbrink et al., 2006, Niimi et
119 al., 2017, Kim et al., 2019), we define the requirement for FOXO1 in the remodeling vasculature
120 of the early embryonic yolk sac.

121 Herein, we demonstrate a novel role for FOXO1 in regulating AV identity in the murine
122 YS vasculature. Using conditional, endothelial-specific *FoxO1* loss-of-function mutants, we
123 identified a significant down regulation of arterial gene expression in the mouse yolk sac prior to
124 the onset of blood flow. We also detected a significant reduction in *Vegfr2/Fik1* transcripts, but
125 normal expression levels for other pan-endothelial genes such as *Pecam1*, indicating that the
126 formation of ECs is not disrupted but rather VEGF signaling is affected. Using a novel *Dll4*
127 arterial reporter line, we showed that *FoxO1* is required for *Dll4* expression in the murine yolk
128 sac, but not in the embryo proper. Further analysis showed that FOXO1 represses expression
129 of *Sprouty* genes, which encode inhibitors of Raf/MEK/ERK signaling downstream of FGF and
130 VEGF receptor activation. Sprouty factors also modulate angiogenesis by negatively regulating
131 small vessel branching, as well as repressing endothelial cell migration (Gong et al., 2013,
132 Wietecha et al., 2011, Lee et al., 2001). While some have shown that FOXO1 positively
133 regulates *Sprouty* gene expression (Paik et al., 2007), our studies demonstrate that *FoxO1* loss
134 increased *Sprouty2* and *4* mRNA levels, suggesting that FOXO1 represses *Sprouty2/4* in the
135 murine yolk sac. We went on to find that *Sprouty4* overexpression throughout the yolk sac and
136 embryo profoundly altered arterial gene expression in the yolk sac but, similar to early *FoxO1*

137 loss, had an insignificant effect on these transcripts in the embryo proper. Taken together, these
138 data highlight a novel role for FOXO1 in regulating arteriovenous specification in the early yolk
139 sac and reveal a new mechanism wherein FOXO1 represses *Sprouty* gene expression and
140 downstream signaling in the endothelium.

141

142 **Results:**

143 **Defective yolk sac vascular remodeling in *FoxO1*^{ECKO} embryos is not due to abnormalities** 144 **in hemodynamic force or allantois defects**

145 To define the role of FOXO1 in ECs within the early embryo, we conditionally ablated
146 *FoxO1* in the endothelium by crossing *FoxO1*^{flox} mice (Paik et al., 2007) with *Tie2-Cre*
147 transgenic mice, in which Cre recombinase is expressed in endothelial and hematopoietic cells
148 and progenitors starting at E7.5 (Kisanuki et al., 2001). The efficiency of the *Tie2-Cre* mediated
149 recombination of the *FoxO1*^{flox} allele was confirmed by qRT-PCR, which showed over 60%
150 reduction in *FoxO1* mRNA in CKO yolk sacs compared to control littermates at E8.5 (Figure
151 1A). We observed gross phenotypes similar to previous reports (Figure 1B and C and S1A and
152 B) (Sengupta et al., 2012, Furuyama et al., 2004, Hosaka et al., 2004). There were no visible
153 differences in vascular morphology or embryo size between control (*Tie2-Cre*^{+/+};*FoxO*^{+/flox}) and
154 endothelial conditional knockout embryos (*Tie2-Cre*^{+/tg};*FoxO1*^{flox/flox}, hereafter referred to as
155 *FoxO1*^{ECKO}) at E8.5 (Figures 1D and E). However, at E9.5 and E10.5, while the primitive
156 vascular plexus of the control yolk sac had remodeled into a hierarchy of large caliber vessels
157 iteratively branching into smaller diameter capillaries, *FoxO1*^{ECKO} yolk sacs retained a primitive
158 vascular plexus (Figures 1F-I). *FoxO1*^{ECKO} embryos stained with anti-CD31 antibodies showed a
159 thinner and less branched vitelline vein and artery compared to controls (Figure 1J). At E9.5,
160 mutant embryos were reduced in overall size compared to control littermates (Figures 1F and
161 G), and this became more evident at E10.5 (Figures 1B-C, H-I). Additionally, in both E9.5 (not
162 shown) and E10.5 *FoxO1*^{ECKO} embryos (Figure 1I), the pericardial sac was enlarged, and blood

163 was abnormally pooled in the heart. Overall, phenotypes in *FoxO1* mutant embryos are highly
164 reproducible and our observations align well with previously published studies (Sengupta et al.,
165 2012, Furuyama et al., 2004, Hosaka et al., 2004).

166 The appearance of pericardial edema in *FoxO1^{ECKO}* embryos is suggestive of heart
167 failure and compromised circulation. To determine if and when blood flow was impaired, we
168 crossed a primitive erythrocyte transgenic fluorescent reporter line, *ε-globin-KGFP* (Dyer et al.,
169 2001) into the *FoxO1^{ECKO}* background. Live imaging of cultured embryos and high-speed
170 confocal microscopy was used to track individual KGFP labeled erythroblasts to determine
171 blood velocity (Figure 2) (Jones et al., 2004). At E8.5, both control and *FoxO1^{ECKO}* embryonic
172 vessels were filled with blood and erythrocytes moved with a steady directional flow with similar
173 periodicity and velocity (Figures 2A, B, E, and G). By E9.5, control embryos had clearly
174 remodeled vessels, blood flow velocity greater than 700 $\mu\text{m/s}$, and a defined wave pattern with
175 periodicity of 400 ms (Figures 2C and F). However, *FoxO1^{ECKO}* embryos vessels were not
176 remodeled, and blood flow had a significantly lower velocity, with a poorly defined wave pattern
177 (Figures 2D and H). Quantification of blood velocity (Figures 2I-J) and heart rate (Figures 2K-L)
178 revealed no statistical difference in E8.5 control and *FoxO1^{ECKO}* embryos (Figures 2I and K).
179 However, by E9.5, blood velocity and heart rate were significantly decreased in *FoxO1^{ECKO}*
180 embryos (Figures 2J and L), indicating heart failure was occurring in embryos with un-
181 remodeled vessels. Thus, flow initiates normally in *FoxO1^{ECKO}* embryos and flow abnormalities
182 are not detected until after defects in vessel remodeling are evident. Given these results, we
183 restricted our analysis, whenever possible, to E8.25-E8.5 embryos so that poor blood flow did
184 not influence our observations.

185 A previous report on the role of *FoxO1* in placental development described phenotypes
186 including swollen or hydropic allantois, failed chorion-allantoic fusion, and increased cell death
187 in the allantois (Ferdous et al., 2011). Since the previous study was conducted in germline
188 *FoxO1* null embryos, we examined the allantois in global null and *FoxO1^{ECKO}* mutants. While

189 germline *FoxO1* mutants exhibited partially penetrant defects in allantois formation and fusion,
190 these phenotypes were not evident in *FoxO1*^{ECKO} embryos at E9.5 (Table 1). However, both
191 germline and *FoxO1*^{ECKO} embryos show defects in yolk sac vascular remodeling, heart failure
192 phenotypes, and lethality by E11.5. Taken together, these results support a cell autonomous
193 requirement for FOXO1 in yolk sac vessel remodeling and suggest that published cardiac and
194 blood flow defects are secondary to the impaired remodeling of yolk sac vasculature.

195

196 **FOXO1 is necessary to maintain *Flk1/Vegfr2* expression in E8.25 embryos**

197 To further assess the effect of endothelial-specific *FoxO1* deletion in the developing embryo, we
198 examined transcript levels of genes normally expressed in blood vessels by qRT-PCR within
199 *FoxO1*^{ECKO} E8.25 yolk sacs. We focused these experiments at E8.25 to avoid potential
200 complications of later stage heart failure. We observed a significant decrease in *Flk1/Vegfr2*
201 expression in *FoxO1*^{ECKO} yolk sacs, while other pan-endothelial markers such as *Pecam1*, *Tie2*,
202 *VE-Cadherin*, *Flt1/Vegfr1*, and *Cx43* were not significantly affected (Figure 3A). Immuno-
203 labeling of endogenous *Flk1* showed a similar reduction in expression in *FoxO1*^{ECKO} yolk sac
204 endothelial cells at E8.25, while *Pecam1* (CD31) expression – a pan endothelial cell marker –
205 appeared unaffected (Figure 3B). We further confirmed the reduction in *Flk1* expression using
206 magnetic-activated cell sorting (MACS) to isolate CD31⁺ ECs from E8.25 WT and *FoxO1*
207 germline deletion mutant yolk sacs. CD31⁺ yolk sac ECs showed seven-fold higher expression
208 of *Pecam1* mRNA (which encodes CD31) than whole yolk sacs (isolated separately then
209 combined) and approximately thirty-fold higher than the non-endothelial population (CD31⁻),
210 demonstrating the enrichment of endothelial cells via MACS (Figure 3C). To compare WT and
211 mutant endothelial cells, we assayed transcript levels of both *Pecam1* (CD31) and *Flk1* (*Vegfr2*)
212 in the CD31⁺ populations. *Pecam1* levels were comparable between WT and mutant endothelial
213 cells, whereas *Flk1* was significantly reduced in the germline mutant endothelial cells (Figure 3D
214 and E). Finally, we examined *Flk1* expression using a transgenic reporter, *Flk1-H2B::YFP*

215 (Fraser et al., 2005), which labels endothelial cell nuclei. At E8.25, YFP⁺ endothelial nuclei were
216 evenly dispersed throughout the vascular plexus of control yolk sacs, however, the number of
217 YFP⁺ nuclei within the *FoxO1^{ECKO}* yolk sacs were significantly reduced (Figure 3F). The total
218 number of DAPI⁺ nuclei was unchanged. Nuclear segmentation and quantification of the
219 average YFP⁺ cell density revealed a significant reduction in the number of YFP⁺ cells in
220 *FoxO1^{ECKO}* yolk sacs compared to controls (Figure 3G). To determine if the reduction in YFP⁺
221 cells was due to a difference in apoptosis or proliferation, *FoxO1^{ECKO}* litters positive for the *Flk1-*
222 *H2B-YFP* reporter were immunostained for phospho-histone 3 (PH3) or Caspase 3 (Figure 3H
223 and I). We found that neither cell proliferation nor apoptosis within the yolk sac differed
224 significantly between control and *FoxO1^{ECKO}* embryos (Figures 3 H, I, S2A-D). Since the mRNA
225 expression of pan-endothelial markers was not decreased, but *Flk1* transcripts and protein were
226 reduced, we concluded that the low density in YFP⁺ cells is not due to reduced EC numbers, but
227 rather reduced expression of the *Flk1* reporter. Collectively, these data indicate that FOXO1 is
228 required to maintain cell autonomous *Flk1/Vegfr2* expression in ECs, but not required for the
229 formation, proliferation or survival of ECs or the expression of other pan-endothelial markers.

230

231 **FOXO1 is required to regulate arterial gene expression in the yolk sac vasculature**

232 Given the reduction in *Flk1/Vegfr2* expression in E8.25 embryos, and the critical role of VEGF-
233 VEGFR2 signaling in establishing arteriovenous identity in the early embryonic endothelium, we
234 next examined other markers of AV specification (Figure 4A). Previously, Furuyama *et al.*
235 showed reduced expression of the arterial-enriched transcripts *Cx40*, *Cx37*, *eNOS*, and
236 *EphrinB2* in the yolk sacs of E9.5 *FoxO1^{ECKO}* mutants compared to control littermates
237 (Furuyama et al., 2004), but given the changes in blood flow that we observed in E9.5
238 *FoxO1^{ECKO}* embryos, we were interested to determine if expression of these markers was
239 affected earlier. Indeed, these genes were significantly reduced in *FoxO1^{ECKO}* yolk sacs at
240 E8.25 compared to controls (Figure 4A). In addition, we found a significant reduction in

241 transcript levels of Notch family members, including *Notch1*, *Hey1*, *Hey2*, *Jagged1* and *Dll4*,
242 which are required for arterial specification (Gridley, 2010, Duarte et al., 2004, Xue et al., 1999,
243 Fischer et al., 2004). Furthermore, *Neuropilin1*, which encodes a co-receptor for VEGFR2 and is
244 required for arterial specification, was also downregulated, whereas its venous counterpart,
245 *Neuropilin2*, remained unchanged (Herzog et al., 2001). Additional venous markers, *Coup-TFII*
246 (*NR2F2*) and *EphB4*, showed a modest decrease, or no significant change, respectively (Wang
247 et al., 1998, You et al., 2005). The endodermal marker *Afp* was also unchanged (Figure 4A)
248 (Dziadek and Adamson, 1978), showing further that gene transcription changes were confined
249 to markers in the arterial endothelium. These results demonstrate that FOXO1 is required for
250 normal expression of early arterial genes, but is dispensable for venous identity, in the murine
251 yolk sac.

252 To determine if reduced transcript levels of arterial-specific genes correlated with
253 decreased expression of their respective proteins in *FoxO1^{ECKO}* yolk sacs, immunofluorescence
254 was performed on sectioned yolk sacs at E8.25. Confocal imaging of Cx37 and Cx40 revealed
255 an overall reduction in the number of connexin-positive puncta in *FoxO1^{ECKO}* yolk sacs when
256 compared to controls (Figure S3A and B). Similarly, we observed decreased eNOS expression
257 within the vascular plexus in *FoxO1^{ECKO}* yolk sacs compared to controls (Figure 4B). These
258 data, in addition to previous gene expression analysis, indicate that FOXO1 within the
259 developing endothelium is necessary for the regulation of arterial endothelial cell identity.

260

261 **Characterization of arterial defects in *FoxO1^{ECKO}* and germline mutants using the *Dll4-*** 262 ***BAC-nlacZ* reporter**

263 Thus far, our phenotypic, transcriptional, and immunolabeling studies support a role for FOXO1
264 as a regulator of vascular remodeling, *Flk1* expression and arterial specification of endothelial
265 cells within the yolk sac. To further analyze the arterial specification defects in *FoxO1^{ECKO}*
266 mutants, we examined the spatial expression of one of the earliest markers of arterial identity

267 (Chong et al., 2011, Wythe et al., 2013), *Dll4*, using a transgenic reporter line, *Dll4-BAC-nlacZ*,
268 that faithfully recapitulates endogenous *Dll4* expression (Herman et al., 2018). E8.25 *FoxO1^{ECKO}*
269 embryos carrying the nuclear-localized β -galactosidase reporter were compared with control
270 littermates (Figure 5). In E8.25 control embryos, *Dll4-BAC-nlacZ* reporter activity was observed
271 in the dorsal aorta (DA), endocardium (EC), and nascent umbilical artery (UA) within the
272 allantois (Figure 5A and S4A). LacZ positive nuclei were also detected within the YS in and
273 around the vitelline artery and arterioles (Figure 5A, red arrows). *FoxO1^{ECKO}* yolk sacs exhibited
274 a similar LacZ expression pattern spatially, albeit with reduced intensity (Figure 5B), consistent
275 with our transcript analysis showing reduced *Dll4* mRNA expression in the *FoxO1^{ECKO}* yolk sacs
276 (Figure 4A and 5C). However, unlike in the yolk sac, nLacZ expression was only slightly
277 reduced in the embryo proper of *FoxO1^{ECKO}* mutants (Figure S4B compared to S4A, Figure 5C).
278 To determine if the differences in nLacZ reporter expression between the yolk sac and embryo
279 was influenced by Cre-mediated recombination in our conditional knockout studies, we
280 examined the activity of the *Dll4* LacZ reporter in germline *FoxO1* mutants. Figures 4SE and F
281 show representative images of anterior views of the embryos, while Figure 5D and E show
282 posterior views. Results similar to the findings in the *FoxO1^{ECKO}* embryos were observed, but
283 with even greater decreases in reporter expression between control (5D red arrows) and null
284 (5E red arrows) yolk sacs and embryos. Endogenous *Dll4* expression in the embryo proper and
285 the yolk sac showed a small, but significant decrease in endogenous *Dll4* expression between
286 control and *FoxO1* null embryos. Comparatively, a dramatic reduction in *Dll4* expression was
287 observed in the *FoxO1* null yolk sacs compared to wildtype controls (Figure 5F).

288 By E9.5, nLacZ reporter expression was detected in the arterial tree in the yolk sac,
289 particularly in the VA and within the arterioles (Figure 5G and 5G inset). Consistent with the
290 E8.25 results, we found *Dll4* expression reduced in E9.5 *FoxO1^{ECKO}* yolk sacs (Figure 5H and
291 5H inset) but strong expression in vessels within control and *FoxO1^{ECKO}* embryos (Figures 5I
292 and J). Germline null embryos showed similar nLacZ activity compared to controls (Figure 5K),

293 but reporter expression was not detectable in null yolk sacs, despite the strong expression seen
294 in the embryo (5L). Isolated embryos confirmed LacZ expression in both control (5M) and null
295 embryos (5N). Additional analysis of *Dll4* reporter expression confirmed previous reports of
296 vascular defects in *FoxO1* mutants, including within the intersomitic vessels, cranial vessels and
297 dorsal aorta (5I, J,M, and N, red arrows) (Hosaka et al., 2004, Ferdous et al., 2011,
298 Dharaneeswaran et al., 2014). Collectively, our results indicate that FOXO1 plays a critical and
299 early role in the regulation of *Dll4* expression, a key factor in determining arterial identity, within
300 the extra-embryonic arteries of the yolk sac, but does not appear to be required for *Dll4*
301 expression within the embryo proper.

302

303 ***FoxO1* deletion in endothelial cells upregulates *Sprouty2/4* expression**

304 We uncovered a novel role for FOXO1 in the establishment of arterial identity, but neither *Fik1*
305 nor *Dll4* contain known binding sites for FOXO1, so we examined expression levels of
306 previously validated FOXO1 direct transcriptional targets in the endothelium: adrenomedullin
307 (*Adm*), BMP binding endothelial regulator (*Bmper*), *eNOS*, *Sprouty2*, and *Vcam1* (Potente et al.,
308 2005, Ferdous et al., 2011). qRT-PCR analysis in *FoxO1^{ECKO}* yolk sacs at E8.25 (Figure 6A)
309 revealed no significant reduction in *Adm* or *Bmper*, but a significant downregulation in *eNOS*
310 and *Vcam1*, as previously described in other tissues (Potente et al., 2005, Ferdous et al., 2011).
311 Interestingly, *FoxO1^{ECKO}* yolk sacs showed significantly increased *Sprouty2* expression (Figure
312 6A). Subsequent analysis showed that in addition to *Sprouty2*, *Sprouty4* was also upregulated
313 in mutant yolk sacs compared to controls, while *Sprouty1* and 3 levels were unchanged (Figure
314 6B). We focused our subsequent analysis on the Sprouty factors because Sprouty4 over-
315 expression had been shown to inhibit angiogenesis in the yolk sac (Lee et al., 2001) and the
316 upregulation of *Sprouty* transcripts led us to hypothesize that FOXO1 may act as a direct
317 repressor of *Sprouty* gene expression.

318 In keeping with the idea that FOXO1 may normally repress *Sprouty 2/4* transcription, we
319 examined endogenous mRNA levels of *FoxO1* and *Sprouty1-4* in wildtype E8.25-8.5 yolk sacs.
320 This analysis revealed that *Sprouty2/4* expression is much lower than *FoxO1*, *Sprouty1* or
321 *Sprouty3* (Figure 6C). To expand and confirm our previous analysis of *Sprouty 2/4* expression,
322 we examined *Sprouty 2/4* transcripts in CD31⁺ and CD31⁻ MACS-sorted ECs from germline
323 *FoxO1* mutants and controls (Figure 3D). For *Sprouty2*, we observed increased expression in
324 CD31⁺ cells, but there was no change in non-endothelial cells from null mutant yolk sacs (Figure
325 6D). Surprisingly, while *Sprouty4* transcripts increased in ECs of null yolk sacs, transcripts were
326 decreased in non-endothelial cells. These data suggest that FOXO1 may act as both a
327 transcriptional repressor or activator in adjacent tissues in the yolk sac, depending on the cell
328 identity or transcriptional target.

329

330 **FOXO1 directly binds to endogenous *Sprouty2/4* promoters and represses *Sprouty2/4*** 331 **transcription**

332 FOXO1 is known to regulate *Sprouty2* mRNA expression in liver endothelial cells, and *in vivo*
333 chromatin immunoprecipitation (ChIP) experiments confirmed that FOXO1 occupies four
334 conserved FOXO binding elements within the murine *Sprouty2* locus (Paik et al., 2007). The
335 first FOXO1 binding site (Figure S5A) is located ~4kb upstream of the transcriptional start site
336 (TSS) of murine *Sprouty2*, and the second DNA-binding site is within exon 2 (Figure 7A). The
337 third and fourth FOXO1 binding sites are located ~5kb and 7kb downstream of the TSS,
338 respectively (Figure 7A). Paik, et al. showed that FOXO1 interacts with these loci to activate
339 *Sprouty2* in the liver, but it was unknown whether FOXO1 utilizes the same binding sites to
340 repress *Sprouty2* in the yolk sac. To determine if FOXO1 occupies any of these four identified
341 binding sites in the murine yolk sac, we performed ChIP-PCR using pooled E8.25 yolk sacs. As
342 shown in Figure 7B, FOXO1 occupancy was significantly enriched at the -4051, +5060, and
343 +6972 regions compared to IgG control. FOXO1 enrichment was not observed at the +4479

344 region. This demonstrates that during early yolk sac blood vessel development, FOXO1 binds
345 *Sprouty2* at regulatory regions -4051, +5060, and +6972 and supports the context-dependent
346 function of FOXO1.

347 Next, we generated luciferase reporter constructs containing ~2kb of the murine
348 *Sprouty2* promoter, or specific regulatory regions harboring FOXO1 binding sites, and
349 measured transcriptional activity in cultured mammalian cells (Figure S5B). To avoid potential
350 confounds in our analysis from endogenous FOXO1, the human lung cancer cell line H1299
351 was chosen since FOXO1 protein expression is undetectable in this line (Zhao et al., 2010).
352 Overexpression of *FoxO1* (*FLAG::FoxO1*) significantly repressed luciferase activity of the
353 promoter construct containing the -4051 FOXO1 binding site in a dose dependent manner.
354 Furthermore, co-transfecting the same reporter construct along with a FOXO1 cDNA without
355 a DNA binding domain abolished this transcriptional repression (Figure 7C). In contrast,
356 FOXO1 did not significantly repress luciferase activity in the constructs containing either the
357 +4479/5060 or +6972 *Sprouty2* regulatory regions. These results suggest that FOXO1 directly
358 downregulates *Sprouty2* expression via the -4051 site in its promoter.

359 To determine if this role for FOXO1 is evolutionarily conserved, we examined the
360 *Sprouty4* locus for conserved FOXO1 DNA-binding motifs. Two putative binding sites, which
361 were conserved in at least three vertebrate genomes (mammalian and non-mammalian),
362 were identified +8755 bp and +14942 bp downstream of the *Sprouty4* TSS (Figure 7D).
363 FOXO1 ChIP-PCR using E8.25 yolk sac chromatin showed a significant enrichment of
364 FOXO1 occupancy in both regulatory regions (Figure 7E). Luciferase assays in H1299 cells
365 also showed that these same sites were required for wildtype FOXO1 dose-dependent
366 repression of reporter activity (Figure 5F; S5E). Taken together, data from the *Sprouty* mRNA
367 expression analysis, as well as ChIP and luciferase assays, demonstrated that FOXO1
368 directly repressed *Sprouty2* and *Sprouty4* transcription in the E8.25 murine yolk sac via
369 known and newly identified conserved DNA-binding sites.

370

371 **Transient overexpression of *Sprouty4* in endothelial cells phenocopies conditional**
372 **loss-of-function *FoxO1* mutants**

373 Given the fact that *Sprouty2* and *Sprouty4* are known to have anti-angiogenic functions
374 (Taniguchi et al., 2009, Wietecha et al., 2011, Lee et al., 2001), and our data herein show that
375 FOXO1 directly represses *Sprouty2/4* expression in the yolk sac, we hypothesized that FOXO1
376 promotes arterial gene expression by repressing *Sprouty2/4*. It had previously been shown that
377 adenovirus-mediated overexpression of *Sprouty4* in developing embryos inhibited sprouting and
378 branching of small vessels in the embryo proper and vessel remodeling in the yolk sac (Lee et
379 al., 2001). To test whether *Sprouty4* overexpression could recapitulate the *FoxO1* loss-of-
380 function phenotype, we utilized a well-characterized *Flk1* promoter-enhancer construct (Kappel
381 et al., 1999, Ronicke et al., 1996, Fraser et al., 2005) to transiently overexpress *Sprouty4* in the
382 endothelial cells of the mouse embryo and YS beginning at E7.5. To track transgene
383 expression, a H2B::YFP reporter was inserted downstream to enable identification of YFP⁺
384 transgenic embryos (schematized in Figure 8A). E8.25 or E9.5 yolk sacs of YFP⁺ transgenic
385 embryos (n=3) showed poorly remodeled vasculature, as their vessels remained as a primitive
386 vascular plexus, while at E9.5 non-transgenic embryos had a normally developed vitelline artery
387 with large caliber vessels branching into smaller diameter capillaries (Figure 8B). The lack of
388 yolk sac vascular remodeling in the transient transgenic *Flk1-Sprouty4* embryos phenocopied
389 the *FoxO1*^{ECKO} embryos and was similar to previous loss of function data (Lee et al., 2001). Yolk
390 sacs harvested from both transgenic and control embryos confirmed the expression of
391 exogenous *Sprouty4* and detection of YFP transcripts only in transgenic embryos (Figure S6).

392 Next, we collected total RNA from E8.25 transgenic YFP⁺ and control yolk sacs and
393 embryos for analysis of arterial marker genes. The relative expression level of each arterial
394 marker was normalized to relative endogenous *Sprouty4* in order to compare the effect of
395 exogenous *Sprouty4* overexpression, and then compared between control and YFP⁺ transgenic

396 groups. Arterial markers, such as *Cx37*, *EphrinB2*, *Notch1*, *Hey1*, *Jagged1*, and *Dll4* were
397 significantly downregulated in the yolk sacs of transgenic embryos compared to controls (Figure
398 8C), while expression within the embryo proper of these markers was not significantly changed,
399 with the exception of *Jagged1* (Figure 8D). The expression of *Cx40* was not significantly
400 different between the control and transgenic groups in either the yolk sac or embryos (Figures
401 8C and D). Additionally, unlike in *FoxO1^{ECKO}* yolk sacs, expression of venous marker *EphB4*
402 was significantly down regulated in the yolk sac and *Coup-TFII* expression was significantly
403 increased in the transgenic embryos, suggesting that either *Sprouty4* could have FOXO1
404 independent functions, or that abnormally high levels of *Sprouty4* may affect other processes.
405 These data, combined with our results showing that FOXO1 represses *Sprouty2/4* transcription,
406 indicates that FOXO1 acts as a key transcriptional regulator in arterial-venous specification by
407 repressing an antagonist of arterial specification.

408

409 **DISCUSSION**

410 Previously, using either through germline mutations or conditional approaches, several groups
411 demonstrated a requirement for FOXO1 in the early embryo, as these mutants featured failed
412 yolk sac remodeling and mid-gestation lethality (Sengupta et al., 2012, Furuyama et al., 2004,
413 Hosaka et al., 2004). In this paper, we investigated the role of FOXO1 within endothelial cells
414 prior to the onset of consistent circulation and overt vascular remodeling. It is well known that
415 arteriovenous specification and the arterial gene expression program are influenced by
416 hemodynamic forces (le Noble et al., 2004, le Noble et al., 2005, Wragg et al., 2014), but our
417 goal here was to determine whether FOXO1 functions in the endothelium before the onset of
418 hemodynamic signaling to affect arteriovenous patterning. Herein, we demonstrate that blood
419 flow is normal in *FoxO1^{ECKO}* mutants at these early stages, although heart failure and poor
420 circulation are evident by E9.5 (Figure 2). Others have shown that FOXO1 is not required for
421 heart development (Sengupta et al., 2012), and it is possible that heart failure in these embryos

422 is caused by the increased resistance of blood flow encountered in the unremodeled vitelline
423 vessels. It has also been noted that loss of FOXO1 causes allantois defects, preventing normal
424 allantois fusion and circulation to the placenta (Ferdous et al., 2011). We did not observe overt
425 defects in allantois fusion in *FoxO1^{ECKO}* embryos (0/10 *FoxO1^{flox/flox};Tie2-cre^{Tg/+}*) (Table 1) and
426 observed only low penetrance of allantois fusion defects in (2/15) in the germline *FoxO1* knock
427 out embryos, whereas 100% of all null or *FoxO1^{ECKO}* embryos examined showed defects in yolk
428 sac remodeling, heart failure and mid-gestation lethality. Thus, it is likely that the heart failure
429 and lethality are caused by increased resistance to blood flow in vitelline vessels; however, the
430 reduction in *Dll4* expression that we observed using the *Dll4-BAC-nlacZ* reporter in *FoxO1^{ECKO}*
431 and germline null mutants suggest that further investigation of the consequence *Dll4* loss in
432 allantois development is warranted.

433 In this study, we report that FOXO1 plays a previously unidentified role in regulating
434 arterial-specific gene expression prior to the onset of blood flow. Based on transcript expression
435 analyses, antibody immunostaining, and transgenic murine reporter experiments, we have
436 concluded that loss of *FoxO1* causes a significant downregulation in *Fik1* and other critical
437 arterial markers, including *Dll4*, in YS endothelial cells without affecting cell proliferation or cell
438 death. Further, our data demonstrate that FOXO1 directly binds to regulatory regions of *Sprouty*
439 2 and 4 in the yolk sac, and that FOXO1 acts as a direct repressor of *Sprouty 2* and 4 in
440 endothelial cells. Finally, we show that the overexpression of *Sprouty4* in endothelial cells *in*
441 *vivo* was sufficient to recapitulate impairments in both vascular remodeling and arterial cell fate
442 specification seen in *FoxO1* mutants. Thus, these data indicate that repression of *Sprouty2/4* by
443 FOXO1 is required to promote early, specification of arterial identity in the yolk sac prior to the
444 onset of robust embryonic circulation.

445 Interestingly, although we observed elevated *Sprouty 2/4* transcripts in yolk sac
446 endothelial cells of *FoxO1* null embryos, we found reduced *Sprouty 4* mRNA expression in non-
447 endothelial cells (CD31-) in the yolk sac, suggesting FOXO1 may act as activator for *Sprouty 4*

448 in other cell types of the yolk sac. Several recent studies have shown that FOXO1 functions as
449 a transcriptional repressor in hepatocytes (Langlet et al., 2017) and pancreatic progenitor cells
450 (Jiang et al., 2017). Interestingly, in some instances co-factors have been identified that enable
451 FOXO1 to act as an activator or a repressor within the same tissues (Langlet et al., 2017). A
452 similar mechanism may explain the observed differences between endothelial and non-
453 endothelial cells within the yolk sac. It is not yet known whether a transcriptional co-factor in YS
454 endothelial cells is required for FOXO1 to act as a repressor, or if another mechanism accounts
455 for the opposite regulation of *Sprouty_4* in adjacent cell layers.

456 *FoxO1* loss did not appear to effect normal expression of pan-endothelial markers
457 *Pecam1*, *Tie2*, and other genes, but *Flk1/Vegfr2* was significantly reduced in both *FoxO1*^{ECKO}
458 and sorted germline mutant yolk sac endothelial cells. We also found that despite the reduction
459 in *Flk1/Vegfr2*, we did not observe changes in cell proliferation or cell viability, two process that
460 are directly regulated by VEGF-VEGFR signaling (Bernatchez et al., 1999). Sprouty factors
461 inhibit receptor tyrosine kinase (RTK) signaling, and Sprouty overexpression could cause a
462 reduction in *Flk1/Vegfr2* that is normally promoted by FLK1 or FGF receptor activation (Lee et
463 al., 2001, Casci et al., 1999). Indeed, we observed a reduction in *Flk1* transcripts when
464 *Sprouty4* was overexpressed in transgenic embryos, but also observed a strong effect on the
465 expression of other endothelial markers such as *Pecam*. It is also possible that the reduction of
466 *Flk1* expression seen in *FoxO1* mutants is a secondary consequence of disrupted arterial
467 specification, rather than a primary driver of this defect.

468 *Dll4* is among the earliest markers of arterial gene expression (Chong et al., 2011,
469 Wythe et al., 2013), but precisely how *Dll4* expression is initiated within the early yolk sac and
470 embryo remains poorly understood. While *Dll4* transcription was suggested to be regulated by 5'
471 binding of FOXC1/2 and β -catenin in its proximal promoter (Corada et al., 2010, Hayashi and
472 Kume, 2008, Seo et al., 2006), subsequent *in vivo* analysis showed that this region is not
473 sufficient to mediate expression (Wythe et al., 2013). Additionally, endothelial-specific loss of β -

474 *catenin* failed to alter *Dll4* expression in mice, or produce arteriovenous patterning defects
475 (Wythe et al., 2013). Furthermore, functional enhancers were found within intron 3 and
476 upstream at -12 and -16 kb that recapitulated the pattern of endogenous *Dll4* expression
477 (Sacilotto et al., 2013, Wythe et al., 2013), and these regions lacked conserved FOXC1/C2
478 binding sites, as well as TCF/LEF binding sites. In these current studies, we used a nuclear
479 localized LacZ reporter that recapitulates the normal expression pattern of *Dll4* (Herman et al.,
480 2018). Our data clearly showed that the reduction in *Dll4* expression was far more severe in the
481 yolk sac of *FoxO1^{ECKO}* or null embryos than within the embryo proper. Similarly, the
482 overexpression of *Sprouty 4* throughout the embryo and yolk sac using an endothelial-specific
483 *Vegfr2/Flk1* promoter (Kappel et al., 1999, Ronicke et al., 1996, Fraser et al., 2005) indicated
484 that *Sprouty* overexpression did not alter arterial gene expression in the embryo, but
485 suppressed arterial transcripts in the yolk sac. The mechanism that explains the differential
486 activity of FOXO1 and SPROUTY2/4 within the vasculature of the yolk sac vs the embryo
487 proper remains unclear. Future experiments will be required to address numerous possible
488 explanations including differences in mesodermal cell lineages, differential binding to cofactors
489 and/or differences in post-translational modifications regulated by local cell-cell signaling.

490 One unresolved question from these studies is the relationship between abnormal
491 arteriovenous specification and failed vessel remodeling. Both arteriovenous identity and vessel
492 remodeling are regulated by hemodynamic forces, and AV specification relies on pathways that
493 respond to VEGF signaling (Fish and Wythe, 2015, Covassin et al., 2006, Weinstein and
494 Lawson, 2002, Fang et al., 2017). In *FoxO1^{ECKO}*, we detected a downregulation in
495 Flk1/VEGFR2. VEGFR2 and other VEGF receptors have been shown to act as shear stress
496 mechanosensors, signaling through downstream pathways such as the MEK-ERK kinase
497 cascade in response to changes in blood flow (Tzima et al., 2005, Baeyens and Schwartz,
498 2016). Thus, the downregulation of VEGFR2 in *FoxO1* mutant embryos could prevent ECs from
499 responding to normal blood flow signaling needed for vessel remodeling. Previously, our lab

500 showed that ECs within the vitelline arteries, but not the vitelline veins, migrate directionally in
501 response to hemodynamic changes in the yolk sac vasculature (Udan et al., 2013) so it is
502 possible that the loss of FOXO1 and/or the overexpression of *Sprouty2/4* interferes not only with
503 initial *Dll4* specification, but with the cell's ability to sense mechanical signaling that is necessary
504 to direct cell migration required for remodeling. Further work will be needed to better understand
505 the mechanisms leading both to early *Dll4* expression and those that regulate the cellular
506 responses needed for vessels to adapt to changes in blood flow.

507

508 **EXPERIMENTAL PROCEDURES**

509 **Animals and genotyping**

510 All animal experiments were conducted according to protocols approved by the Institutional
511 Animal Care and Use Committee of Baylor College of Medicine. *Ella-Cre* and *Tie2-Cre*
512 transgenic mice were purchased from Jackson Labs (# 003724 and 008863, respectively). ϵ -
513 *globin-KGFP* (Dyer et al., 2001), *FoxO1^{flox/flox}* mice (Paik et al., 2007), and *Dll4-BAC-nLacZ* mice
514 (Herman et al., 2018) were maintained and genotyped as previously described. *FoxO1* germline
515 knockout mice were generated by crossing the *FoxO1^{flox/flox}* mice to *Ella-Cre* mice (Lakso et al.,
516 1996). *Fik1-H2B::YFP* reporter mice were kindly provided by Dr. K. Hadjantonakis, Memorial
517 Sloan Kettering Cancer Center (Fraser et al., 2005).

518

519 **Immunostaining of whole or sectioned yolk sacs and LacZ staining**

520 E8.25 yolk sacs were fixed in 4% PFA, rinsed in PBS, permeabilized with 0.1% TritonX-100 for
521 1 hour, and blocked in 2% normal donkey serum/1% BSA for 5 hours. Yolk sacs were then
522 incubated with anti-PECAM1 antibody (BD Pharmingen, #550274; 1:100) overnight at 4°C. After
523 several PBS washes, yolk sacs were incubated with goat anti-rabbit antibody (Molecular
524 Probes, AlexaFluor 633,1:500) and DAPI (1:500) overnight at 4°C. Finally, yolk sacs were
525 rinsed in PBS and imaged using the Zeiss LSM510 META confocal microscope. Dissected yolk

526 sacs were cryosectioned at 20 μ m and sections were permeabilized and blocked, and incubated
527 with antibodies to either Caspase 3 (Cell Signaling #9661, 1:50); Connexin37 (ThermoFisher
528 Scientific #404200, 1:50); Connexin40 (ThermoFisher Scientific #364900, 1:50); eNOS (Santa
529 Cruz #sc-654, 1:50); Flk1 (Sigma #V1014, 1:100); or pHistone H3 (Millipore #06-570, 1:50)
530 overnight at 4°C. The secondary antibody incubation and image acquisition were performed as
531 described previously.

532
533 *Dll4-BAC-nLacZ* transgenic reporter were examined on *FoxO1* germline or *FoxO1*^{ECKO} (*Tie2-*
534 *Cre*^{+tg};*FoxO1*^{flloxfllox}) backgrounds. E8.5 and E9.5 embryos were dissected in cold PBS and fixed
535 in 4% PFA. Embryos were then washed in X-gal rinse buffer (0.02% NP40, 0.01% sodium
536 deoxycholate; 4 x 15mins) and thereafter stained in x-gal solution [5mM K₃Fe(CN)₆, 5mM
537 K₄Fe(CN)₆, 0.01% sodium deoxycholate, 0.02% NP40, 2mM MgCl₂, 5mM EGTA, 1mg/ml X-gal]
538 at 37°C overnight. Embryos were then post-fixed in 4% PFA and then cleared in 50% and 70%
539 glycerol. Embryos from the same litter were processed and stained in a 20ml scintillation vial.
540 Stained embryos were photographed using the Axio ZoomV16 (Zeiss) stereo microscope and
541 thereafter genotyped.

542
543 **Quantification of *Fik1-H2B::YFP*⁺ cell density, proliferation index and apoptotic index in**
544 **whole mount yolk sacs using FARSIGHT**

545 Acquired WT and ECKO yolk sac whole mount images (n>3 yolk sacs per genotype, n>3
546 regions of interest per yolk sac) were made into maximum intensity projections and separated
547 into individual RGB images: Red (pHistone-H3/Caspase 3), Green (*Fik1-H2B::YFP*) and Blue
548 (DAPI). Individual nuclei for Red, Green and Blue channels were segmented and quantified
549 using FARSIGHT, courtesy of Badri Roysam, University of Houston, which makes use of both
550 intensity and volume thresholds to distinguish two nuclei as separate. *YFP*⁺ cell density was
551 defined as the ratio of *YFP*⁺ nuclei to DAPI⁺ nuclei within that same field of view.

552 Proliferative/apoptotic index was defined as the ratio of PH3⁺/ Caspase3⁺ nuclei to the number
553 of DAPI⁺ nuclei. Endothelial cell proliferative/apoptotic index was defined as the ratio of
554 YFP⁺;PH3⁺/Caspase3⁺ double positive nuclei to the number of YFP⁺ nuclei. The ratios were then
555 averaged over the various WT and ECKO yolk sac images.

556

557 **Live imaging and analysis of blood flow in *FoxO1* conditional knockout embryos**

558 *ε-globin-KGFP* reporter expressing GFP in primitive erythroblasts was examined in control and
559 ECKO background and litters were dissected at E8.5 or E9.5 for blood velocity analysis.
560 Embryos were dissected under a heated (37°C) dissection stage with warm dissection media
561 (DMEM/F-12, 10% FBS, 100 U/mL penicillin, and 100 µg/mL streptomycin). Embryos with intact
562 ectoplacental cone were placed in a glass bottomed culture chamber with culture medium (1:1
563 DMEM/F-12: rat serum, 100 U/mL penicillin, and 100 µg/mL streptomycin) and allowed to
564 recover in a 37°C incubator for 20 minutes. Embryos were then placed on a heated confocal
565 microscope stage (37°C) and imaged using the Zeiss LSM 5 LIVE laser scanning confocal
566 microscope, using the Achroplan 20X/0.45 NA objective. A 200-frame time lapse (in a 512x512
567 pixel frame) was acquired at 30-50 frames per second. Blood flow time lapses were acquired at
568 three different locations throughout the yolk sac per embryo, and at least three embryos of each
569 genotype were used for data collection. Individual blood cell velocities in each track were
570 determined from time lapse movies using Imaris. Individual blood cell velocities from three
571 different locations per embryo were averaged. Average heart beats per minute were calculated
572 by measuring the average time interval between peak velocities during the course of 5 cardiac
573 cycles in individual velocity profiles for each embryo imaged. Embryos were genotyped after
574 imaging, and blood velocities and heart beats per minute were averaged within WT and ECKO.

575

576 **Magnetic activated cell sorting of yolk sack endothelial cells**

577 To isolate E8.25 yolk sac endothelial cells, fresh yolk sacs were dissected in cold DMEM/F12
578 media without phenol red (ThermoFisher Scientific #21041025), individually placed in 100 μ L of
579 cold TrypsinLE (Fisher Scientific #12605010), and kept on ice until all yolk sacs were harvested.
580 Embryos were used for genotyping. To dissociate yolk sacs into single cell suspension, gently
581 triturate with p200 pipette and incubate on ice for 5 minutes and repeat for a total of four times.
582 To inhibit the enzyme, add 1 mL of stop solution: media + 10% FBS (ThermoFisher Scientific
583 #26140079). The yolk sac cell suspensions were pelleted at 0.8 X 1000g for 5 minutes at 4
584 degrees Celsius. The pellets were resuspended in 90 μ L of cell suspension buffer (PBS + 2%
585 FBS + 2 mM EDTA). 10 μ L of CD31 MicroBeads (Miltenyi Biotec #130-097-418) were added to
586 each yolk sac cell suspension and samples were incubated on ice for 15 minutes in the dark.
587 Cell mixtures were pelleted at 0.8 X 1000g for 5 minutes at 4 degrees Celsius and washed with
588 1mL of cell suspension buffer. Cell mixtures were once again pelleted at 0.8 X 1000g for 5
589 minutes at 4 degrees Celsius and resuspended in 200 μ L of cell suspension buffer. Cell mixtures
590 were passed through 40 μ m cell strainers (Fisher Scientific #352340) into FACS tubes and
591 strainers were washed with 300 μ L of cell suspension buffer. MS columns (Miltenyi Biotec #130-
592 041-301) were placed on OctoMACS separator and prepared according to manufacturer
593 instructions. Cell mixtures were individually passed through columns and the flow through was
594 reapplied through columns to maximize endothelial cell retention (CD31⁺ population). Columns
595 were washed three times with 500 μ L cell suspension buffer and all flow through was collected
596 (CD31⁻ population). Bound cells were released from the columns by removal from magnetic
597 separator, and 1 mL of cell suspension buffer was applied to the columns and cells were flushed
598 using plunger into a 1.5 mL Eppendorf tube. Collected cells were then pelleted at 0.8 X 1000g
599 for 5 minutes at 4 degrees Celsius and resuspended in Trizol (Thermo Fisher 15596018). After
600 genotyping, CD31⁺ and CD31⁻ populations from two yolk sacs were combined and processed

601 for RNA isolation (QIAGEN RNeasy Micro Kit #74004), cDNA synthesis and qRT-qPCR as
602 described below.

603

604 **RNA isolation and qRT-PCR analysis**

605 Total RNA was isolated from pooled E8.25 yolk sacs dissected from either *Tie2-Cre^{+tg}*;
606 *FoxO1^{+flox}* or *Tie2-Cre^{+tg}*; *FoxO1^{flox/flox}* embryos. Purified RNA was reverse transcribed
607 (ThermoFisher Scientific #11752-050) and gene expression analysis was performed using
608 TaqMan real-time assays for *FoxO1*, *Adm*, *Bmper*, *Vcam1*, and a panel of endothelial, arterial,
609 and venous markers (see Fig. 2D, E for gene list). The data were normalized to *Gapdh* (Pfaffl,
610 2001) and relative expression ratios between control and ECKO embryos were determined.
611 Endogenous *FoxO1* and *Sprouty1-4* expression from pooled E8.25 yolk sacs (CD1 strain) was
612 also probed by TaqMan real-time assay, but expression was calculated as fold change relative
613 to *FoxO1*, which was set to 1.

614 Endogenous *Dll4* expression was measured in either germline *FoxO1* knockouts or
615 *FoxO1^{ECKO}* embryos at E8.25. The allantois was used for genotyping and total RNA was
616 extracted from individual embryos and yolk sacs ($n \geq 3$) and probed for *Dll4* expression via
617 TaqMan assay and fold change of expression between controls and homozygous *FoxO1^{ECKO}*
618 mutants, and statistical analysis were performed as described above.

619

620 **Chromatin Immunoprecipitation (ChIP) and qPCR**

621 To determine endogenous FOXO1 chromatin occupancy, E8.25 yolk sacs from CD1 embryos
622 were used for chromatin extraction. Freshly dissected yolk sacs were dissociated in ice cold
623 PBS with protease inhibitors and the tissue was then crosslinked with 1.5% formaldehyde,
624 followed by incubation with 125 mM glycine, and washed with PBS. After centrifugation, the
625 pellet was resuspended in cell lysis buffer (5 mM PIPES, pH 8; 85 mM KCl; 0.5% NP40). The
626 samples were spun and the pellet was resuspended in nuclear lysis buffer (50 mM Tris-HCl, pH

627 8.1; 10 mM EDTA; 1% SDS) and then sonicated on ice using a Bioruptor (Diagenode) to obtain
628 sheared chromatin ranging between 100–500 bp. ChIP was performed according to the
629 instructions for Magna ChIP kit (Millipore #17-10085) using 5 μ g of anti-FOXO1 antibody
630 (Abcam #ab39670) or rabbit IgG (Millipore #12370). The cross links were then reversed, and
631 the purified DNA was then analyzed by qPCR in technical triplicates using SYBR green master
632 mix and the primers listed in Table S1 to measure the percentage of co-precipitating DNA
633 relative to input (% input) in *Sprouty2* and *Sprouty4* genomic regions.

634 635 **Cloning of *mSprouty2/4* promoter constructs and Luciferase Assay**

636 Genomic regions of ~2kb in length of murine *Sprouty2* and *Sprouty4* were PCR amplified using
637 primers listed in Table S1, and using BAC clones of C57BL6 genomic DNA as template DNA
638 (CH29-611D15, CH29-100M12, respectively; CHORI BAC/PAC resources). PCR fragments
639 were ligated into pCRII-TOPO vector, sequenced, and then subcloned into pGL3-Promoter
640 vector (Promega). H1299 cells (ATCC #CRL-5803) were maintained in DMEM media
641 supplemented with 10% FBS, 100 U/ml penicillin, and 100 μ g/ml streptomycin. For transient
642 transfections, 50,000 cells were plated (48-well plate) and after 24 hours, each well was co-
643 transfected with 200 ng of *Sprouty2/Sprouty4* promoter construct, 10 ng of pRL-TK, and 125 ng
644 expression plasmid (pcDNA3-FOXO::FLAG, Addgene #13507) using manufacturer's
645 recommendations for lipofectamine 3000. The total amount of expression plasmid transfected
646 per well was kept constant with varying amounts of pcDNA3.1 vector. As a negative control, a
647 *FoxO1* plasmid encoding a deleted DNA binding domain (amino acid 208-220) was used
648 (Addgene #10694). After 24 hours, cells were lysed and analyzed for firefly and *Renilla*
649 luciferase activities according to the procedure outlined in the Dual-Glo luciferase assay system
650 (Promega #E2920). All luciferase assays were performed in triplicates and repeated at least
651 three times. Student's *t*-test was used to assess statistical significance ($P < 0.05$ was

652 considered statistically significant) and the averages and standard deviation from triplicate
653 samples from representative assays were shown.

654

655 **Transient endothelial-specific *Sprouty* expression in embryos**

656 A mouse *Sprouty4* cDNA clone (TransOmics clone BC057005) was used as a template to PCR
657 amplify the coding sequence with 5' *SacI* and 3' *PmeI* restriction sites (5'
658 GAGCTCCCAGCCTCA TGGAGCCC 3' and 5' GTTTAAACTCAGAAAGGCTTGTCAGAC 3')
659 and subcloned into pCRIITOPO vector (S4-2). The internal ribosome entry site (IRES)
660 sequence was amplified from pIRES-hrGFP1a vector (Agilent Technologies) with 5' *EcoRV* and
661 3' *EcoRI* restriction sites using primers 5' CTATAGATATCACCCCCCTCTCCCTA 3' and 5'
662 GCATGAATTCGGTTGTGGCCATT ATCATCGTG 3' and subcloned into pCRIITOPO vector
663 (IRES-4). To assemble the final transgenic construct, clones S4-2 and IRES-4 were excised
664 with 5' *Ecl136II* and 3' *NotI*, and 5' *NotI* and 3' *Ecl136II*, respectively, and co-ligated into *Flk1*-
665 H2B/EYFP vector (kindly provided by Dr. K. Hadjantonakis, Memorial Sloan Kettering Cancer
666 Center) via a blunt-ended *HindIII* site. The *Flk1*-H2B/EYFP vector has a well characterized *Flk1*
667 promoter and intronic enhancer sequences which drive YFP expression in endothelial cells
668 (Fraser et al., 2005). All clones were verified by DNA sequencing and the final transgenic
669 construct was excised with 5' *SaII* and 3' *XbaI* to purify a 4.5kb fragment for pronuclear
670 microinjection, which was performed at the BCM Genetically Engineered Mouse Core. Transient
671 transgenic embryos were dissected with yolk sac intact and initially screened for YFP
672 expression using confocal microscopy. Gross morphology of the embryo and yolk sac
673 vasculature was examined at E9.5 while arterial marker analysis (*C37*, *Cx40*, *Dll4*, *EphB2*,
674 *Hey1*) was performed at E8.25, at which point embryos and yolk sacs of YFP positive and
675 negative samples (n=3 each) were lysed in Trizol for RNA extraction. Transgene-positive
676 embryos were also confirmed via qRT-PCR for YFP expression (data not shown) and also
677 quantitating the ratio of exogenous over endogenous *mSprouty4* expression using transcript-

678 specific primers. Detection was via the Sybr-green or Taqman assay (for arterial markers) and
679 fold change of expression between YFP-positive and negative samples, and statistical analysis
680 were performed as previously described.

681

682

683 **FIGURE LEGENDS**

684 **Figure 1. *FoxO1*^{ECKO} results in vascular remodeling defects and lethality.** (A) Quantitative
685 RT-PCR for *FoxO1* expression in control and ECKO yolk sacs. $P < 0.01$. (B and C) Bright field
686 images of E10.5 littermate control and *FoxO1*^{ECKO} embryos. Control and *FoxO1*^{ECKO} embryos
687 within the yolk sac at E8.5 (D and E), E9.5 (F and G), and E10.5 (H and I). Pericardial edema
688 (arrow), blood pooling in the heart (asterisk). (J) *Pecam1* staining in E9.5 control and CKO yolk
689 sacs. Scale bar = 500 μ m.

690

691 **Figure 2. Vascular remodeling defects in *FoxO1*^{ECKO} embryos do not result from reduced**
692 **blood flow.** Primitive erythroblasts in circulation in wild type and CKO embryos were marked by
693 crossing to an ϵ -*globin-GFP* transgenic reporter. Representative still images of E8.5 wild type
694 (A), ECKO (B), E9.5 wild type (C), and ECKO (D) embryos. Individual blood cells from A-D
695 were tracked and velocity profiles are plotted in E-H. Quantification of the average blood velocity
696 are graphed in I and J (Mann-Whitney U test, $p = 0.005$). Average heart rates quantified in wild
697 type and ECKO embryos at E8.5 (K) and E9.5 (L) (Kruskal-Wallis test, $p = 0.003$). Bars in graphs
698 are means \pm standard error.

699

700 **Figure 3. FOXO1 regulates FLK1 expression without affecting other endothelial genes or**
701 **endothelial cell viability prior to blood flow.** (A) Expression levels of endothelial genes by
702 quantitative RT-PCR. (B) Yolk sacs from control and *FoxO1*^{ECKO} at E8.25 were DAPI-stained and

703 labelled with *Flk1-H2B::YFP* transgene, which marks the nuclei of endothelial cells
704 (arrowheads). Whole mount phosphoHistone-H3 (PH3) (C) or activated Caspase3 (D) staining
705 of control and *FoxO1^{ECKO}* E8.25 yolk sacs co-labeled with *Flk1-H2B::YFP* transgene and DAPI.
706 (E) Immuno-labeling for endogenous Flk1 and Pecam1 in control and *FoxO1^{ECKO}* yolk sacs.
707 Scale bars = 50 μ m (B -E). (F) Comparison of *Pecam1* expression in MACS sorted CD31-,
708 CD31+, and combined control E8.25 yolk sac cells by qPCR. Relative *Pecam1* (G) and *Flk1* (H)
709 expression between WT and *FoxO1* null E8.25 MACS sorted CD31- and CD31+ yolk sac cells.
710

711 **Figure 4. Arterial marker expression is reduced in *FoxO1^{ECKO}* yolk sac.** (A) Quantitative RT-
712 PCR expression analysis in control and *FoxO1^{ECKO}* yolk sacs; arterial (red), venous (blue), and
713 endoderm markers. * $p < 0.05$, ** $p < 0.01$, *** $p < 0.001$, data are means \pm S.E. (B) Immuno-labeling
714 of eNOS and FLK1 in control and *FoxO1^{ECKO}* yolk sacs. Scale bars = 20 μ m.

715
716 **Figure 5. Characterization of arterial defects in *FoxO1^{ECKO}* and germline mutants using**
717 **the *Dll4-BAC-nlacZ* reporter** (A and B, D and E) *nlacZ* reporter activity was detected in the
718 dorsal aorta [DA] and umbilical artery [UA] in E8.25 control, *FoxO1^{ECKO}*, and *FoxO1* null
719 embryos. Arrowheads point to yolk sac endothelial cells in posterior region of yolk sac plexus.
720 (C and F) *Dll4* expression in control, *FoxO1^{ECKO}*, and *FoxO1* null embryos and yolk sacs. $n > 3$.
721 * $p < 0.05$. (G and H, K and L) *nlacZ* reporter activity in E9.5 control, *FoxO1^{ECKO}*, and *FoxO1* null
722 yolk sac and embryo; VA = vitelline artery [arrow]; insets in G and H show yolk sacs only. (I and
723 J, M and N) *nlacZ* reporter activity in E9.5 control, *FoxO1^{ECKO}*, and *FoxO1* null; EC =
724 endocardium, DA = dorsal aorta, IAV = intersomitic arterial vessels, ACV = arterial cranial
725 vasculature. Scale bars for E8.25 panes = 200 μ m; E9.25 = 500 μ m.

726

727 **Figure 6. FOXO1 regulates *Sprouty2/4* expression in the yolk sac vasculature.** Quantitative
728 RT-PCR analysis in E8.25 control and *FoxO1*^{ECKO} yolk sacs for (A) known FOXO1 targets and
729 (B) *Sprouty* family members. (C) Quantitative RT-PCR of endogenous *Sprouty1-4* expression
730 relative to *FoxO1*. (D) Quantitative RT-PCR of *Sprouty2/4* in MACS sorted E8.25 CD31+ and
731 CD31- control and *FoxO1* null yolk sac cells.

732
733 **Figure 7. FOXO1 directly binds to endogenous *Sprouty2/4* promoters and represses**
734 ***Sprouty2/4* transcription.** (A) Genomic locus of mouse *Sprouty2* gene with FOXO1 binding
735 sites in red. (B and E) FOXO1 ChIP-PCR using E8.25 yolk sac chromatin. (C) Luciferase activity
736 of FOXO1 on *Sprouty2* promoter in H1299 cells. (D) Genomic locus of mouse *Sprouty4* gene
737 with FOXO1 binding sites in red. (F) Luciferase activity of FOXO1 on *Sprouty4* promoter in
738 H1299 cells. * $p < 0.05$, ** $p < 0.01$, *** $p < 0.001$. EV, empty vector.

739
740 **Figure 8. Transient overexpression of *Sprouty4* in endothelial cells phenocopies**
741 **conditional loss-of-function *FoxO1* mutants.** (A) Schematic of *Sprouty4* overexpression
742 construct for pro-nuclei injection. (B) Brightfield image of E9.5 non-transgenic (control) and
743 transgenic embryo (TG); confocal imaging of TG embryo showing YFP fluorescence in yolk
744 sac. Note vessel remodeling in the control yolk sac (arrow). Quantitative RT-PCR of arterial
745 markers in control and TG yolk sacs (C) and embryos (D) (n=3). * $p < 0.05$, ** $p < 0.01$, *** $p < 0.001$.

746
747 **Table 1.** Allantois phenotype analysis in control, null and ECKO embryos at E9.5.

Table S1 Primer sequences used for genotyping, ChIP-qPCR, and cloning

<u>Gene/allele</u>	<u>Primer sequences (5'-3')</u>	<u>Purpose</u>
ChIP <i>mSprouty2</i> (-4051)	TTCCAGTCCTCCAAGCAATCTAG AGTGCCTCCAGGAAGGGAAT	ChIP-qPCR
ChIP <i>mSprouty2</i> (4479)	AATTAGCAAATGGCTCCCGG TTTGTGACTGTGCCATGAAGC	ChIP-qPCR
ChIP <i>mSprouty2</i> (5060)	TAGGGCGACTCAGTGGCTATC GACCGGAGTCAAAGGACCTTC	ChIP-qPCR
ChIP <i>mSprouty2</i> (6972)	CATTTGTGTGTTTTGGGGAGAGAT CGGCAGTTGGGTTGGAATTA	ChIP-qPCR
ChIP <i>mSprouty4</i> (8755)	GATCTCCATCCGAATCCAAATG CTTGGTTCGGCAAAGGCGAGAAAC	ChIP-qPCR
ChIP <i>mSprouty4</i> (14942)	CCACCACAAAAGTTACCACAGAAG GATATCTTCTAGATCAGTAC	ChIP-qPCR
ChIP negative control	GAAACCCGAATCTACATTCCGTTCC CTGGATTAACCCGATTATACACC	ChIP-qPCR
Luc <i>mSprouty2</i> (-4051)	GTGTACACAGGTATACTCTAGTCACCAACCC GGGACTCGATGTTGCAATGAGATACTCAACTC	PCR cloning
Luc <i>mSprouty2</i> (4479/5060)	GATCTGTGACAAGCAGTGCCTCTGCTCAG GCCACAAGGTGACTAATGTTGTCAAGATGG	PCR cloning
Luc <i>mSprouty2</i> (6972)	CATTCAGACCTAGCACTGTGATTCATGC CAGTGTTCAAGCCAAACCAGGTAGGCCTTGA	PCR cloning
Luc <i>mSprouty4</i> (8755)	CAGCGGTTCACTTGAAGCTGCCTTGACAAG CTCTGCCTCCCAACTGCTGGGATTAAAG	PCR cloning
Luc <i>mSprouty4</i> (14942)	CTGTAGCTGTTTCTGACTTCTTGGCTAGC GGCTGAAGACTCATTGTAGAATGGGTCATG	PCR cloning
Endogenous <i>mSpry4 cDNA</i>	GAAGCCTGTCCCTTGGTGCAAGTTCAG CTGGTCAATGGGTAAGATGGTGAGTG	qRT-PCR
Exogenous <i>mSpry4 cDNA</i>	GCGAGGTGCAGGAATTCGTTAAGCTCTCCC CTGGTCAATGGGTAAGATGGTGAGTG	qRT-PCR

748

* pGL3-Promoter

Table S2 Taqman assays for Gene expression analysis

<i>FoxO1</i>	Mm00490672_m1	<i>Hey1</i>	Mm00468865_m1
<i>FoxO3a</i>	Mm01185722_m1	<i>Hey2</i>	Mm00468865_m1
<i>FoxO4</i>	Mm00840140_g1	<i>Jagged 1</i>	Mm00496902_m1
<i>Flk1 (Kdr)</i>	Mm00840140_g1	<i>Nrp1</i>	Mm00435379_m1
<i>PECAM1</i>	Mm01242584_m1	<i>Nrp2</i>	Mm00803099_m1
<i>Tie2 (Tek)</i>	Mm01242584_m1	<i>CoupTFII</i>	Mm00772789_m1
<i>Flt1</i>	Mm00438980_m1	<i>EphB4</i>	Mm01201157_m1
<i>Connexin 43</i>	Mm00438980_m1	<i>AFP</i>	Mm00431715_m1
<i>eNOS</i>	Mm00435217_m1	<i>ADM</i>	Mm00437438_g1
<i>Connexin 37</i>	Mm00433610_s1	<i>BMPER</i>	Mm01175806_m1
<i>EphrinB2</i>	Mm01215897_m1	<i>Sprouty2</i>	Mm00442344_m1
<i>Notch1</i>	Mm00435249_m1	<i>Sprouty4</i>	Mm00442345_m1
<i>Dll4</i>	Mm00444619_m1		

749

750

751 ADAMS, R. H., WILKINSON, G. A., WEISS, C., DIELLA, F., GALE, N. W., DEUTSCH, U.,
752 RISAU, W. & KLEIN, R. 1999. Roles of ephrinB ligands and EphB receptors in
753 cardiovascular development: demarcation of arterial/venous domains, vascular
754 morphogenesis, and sprouting angiogenesis. *Genes Dev*, 13, 295-306.

755 AITSEBAOMO, J., PORTBURY, A. L., SCHISLER, J. C. & PATTERSON, C. 2008. Brothers
756 and sisters: molecular insights into arterial-venous heterogeneity. *Circ Res*, 103, 929-39.

757 ALBERT, P. S., BROWN, S. J. & RIDDLE, D. L. 1981. Sensory control of dauer larva
758 formation in *Caenorhabditis elegans*. *J Comp Neurol*, 198, 435-51.

759 BAEYENS, N. & SCHWARTZ, M. A. 2016. Biomechanics of vascular mechanosensation and
760 remodeling. *Mol Biol Cell*, 27, 7-11.

761 BEARD, R. S., JR., HOETTELS, B. A., MEEGAN, J. E., WERTZ, T. S., CHA, B. J., YANG,
762 X., OXFORD, J. T., WU, M. H. & YUAN, S. Y. 2020. AKT2 maintains brain endothelial
763 claudin-5 expression and selective activation of IR/AKT2/FOXO1-signaling reverses
764 barrier dysfunction. *J Cereb Blood Flow Metab*, 40, 374-391.

765 BERNATCHEZ, P. N., SOKER, S. & SIROIS, M. G. 1999. Vascular endothelial growth factor
766 effect on endothelial cell proliferation, migration, and platelet-activating factor synthesis
767 is Flk-1-dependent. *J Biol Chem*, 274, 31047-54.

768 CASCI, T., VINOS, J. & FREEMAN, M. 1999. Sprouty, an intracellular inhibitor of Ras
769 signaling. *Cell*, 96, 655-65.

770 CHLENCH, S., MECHA DISASSA, N., HOHBERG, M., HOFFMANN, C., POHLKAMP, T.,
771 BEYER, G., BONGRAZIO, M., DA SILVA-AZEVEDO, L., BAUM, O., PRIES, A. R.
772 & ZAKRZEWICZ, A. 2007. Regulation of Foxo-1 and the angiopoietin-2/Tie2 system by
773 shear stress. *FEBS Lett*, 581, 673-80.

774 CHONG, D. C., KOO, Y., XU, K., FU, S. & CLEAVER, O. 2011. Stepwise arteriovenous fate
775 acquisition during mammalian vasculogenesis. *Dev Dyn*, 240, 2153-65.

776 CLEAVER, O. & KRIEG, P. A. 1998. VEGF mediates angioblast migration during development
777 of the dorsal aorta in *Xenopus*. *Development*, 125, 3905-14.

- 778 CORADA, M., NYQVIST, D., ORSENIGO, F., CAPRINI, A., GIAMPIETRO, C., TAKETO,
779 M. M., IRUELA-ARISPE, M. L., ADAMS, R. H. & DEJANA, E. 2010. The Wnt/beta-
780 catenin pathway modulates vascular remodeling and specification by upregulating
781 Dll4/Notch signaling. *Dev Cell*, 18, 938-49.
- 782 COVASSIN, L. D., VILLEFRANC, J. A., KACERGIS, M. C., WEINSTEIN, B. M. &
783 LAWSON, N. D. 2006. Distinct genetic interactions between multiple Vegf receptors are
784 required for development of different blood vessel types in zebrafish. *Proc Natl Acad Sci*
785 *USA*, 103, 6554-9.
- 786 DANG, L. T. H., ABURATANI, T., MARSH, G. A., JOHNSON, B. G., ALIMPERTI, S.,
787 YOON, C. J., HUANG, A., SZAK, S., NAKAGAWA, N., GOMEZ, I., REN, S., READ,
788 S. K., SPARAGES, C., APLIN, A. C., NICOSIA, R. F., CHEN, C., LIGRESTI, G. &
789 DUFFIELD, J. S. 2017. Hyperactive FOXO1 results in lack of tip stalk identity and
790 deficient microvascular regeneration during kidney injury. *Biomaterials*, 141, 314-329.
- 791 DHARANEESWARAN, H., ABID, M. R., YUAN, L., DUPUIS, D., BEELER, D., SPOKES, K.
792 C., JANES, L., SCIUTO, T., KANG, P. M., JAMINET, S. S., DVORAK, A., GRANT,
793 M. A., REGAN, E. R. & AIRD, W. C. 2014. FOXO1-mediated activation of Akt plays a
794 critical role in vascular homeostasis. *Circ Res*, 115, 238-251.
- 795 DICKINSON, M. E., FLENNIKEN, A. M., JI, X., TEBOUL, L., WONG, M. D., WHITE, J. K.,
796 MEEHAN, T. F., WENINGER, W. J., WESTERBERG, H., ADISSU, H., BAKER, C.
797 N., BOWER, L., BROWN, J. M., CADDLE, L. B., CHIARI, F., CLARY, D., CLEAK,
798 J., DALY, M. J., DENEGRE, J. M., DOE, B., DOLAN, M. E., EDIE, S. M., FUCHS, H.,
799 GAILUS-DURNER, V., GALLI, A., GAMBADORO, A., GALLEGOS, J., GUO, S.,
800 HORNER, N. R., HSU, C. W., JOHNSON, S. J., KALAGA, S., KEITH, L. C.,
801 LANOUE, L., LAWSON, T. N., LEK, M., MARK, M., MARSCHALL, S., MASON, J.,
802 MCELWEE, M. L., NEWBIGGING, S., NUTTER, L. M., PETERSON, K. A.,
803 RAMIREZ-SOLIS, R., ROWLAND, D. J., RYDER, E., SAMOCHA, K. E., SEAVITT,
804 J. R., SELLOUM, M., SZOKE-KOVACS, Z., TAMURA, M., TRAINOR, A. G.,
805 TUDOSE, I., WAKANA, S., WARREN, J., WENDLING, O., WEST, D. B., WONG, L.,
806 YOSHIKI, A., INTERNATIONAL MOUSE PHENOTYPING, C., JACKSON, L.,
807 INFRASTRUCTURE NATIONALE PHENOMIN, I. C. D. L. S., CHARLES RIVER, L.,
808 HARWELL, M. R. C., TORONTO CENTRE FOR, P., WELLCOME TRUST SANGER,
809 I., CENTER, R. B., MACARTHUR, D. G., TOCCHINI-VALENTINI, G. P., GAO, X.,
810 FLICEK, P., BRADLEY, A., SKARNES, W. C., JUSTICE, M. J., PARKINSON, H. E.,
811 MOORE, M., WELLS, S., BRAUN, R. E., SVENSON, K. L., DE ANGELIS, M. H.,
812 HERAULT, Y., MOHUN, T., MALLON, A. M., HENKELMAN, R. M., BROWN, S.
813 D., ADAMS, D. J., LLOYD, K. C., MCKERLIE, C., BEAUDET, A. L., BUCAN, M. &
814 MURRAY, S. A. 2016. High-throughput discovery of novel developmental phenotypes.
815 *Nature*, 537, 508-514.
- 816 DIXIT, M., BESS, E., FISSLTHALER, B., HARTEL, F. V., NOLL, T., BUSSE, R. &
817 FLEMING, I. 2008. Shear stress-induced activation of the AMP-activated protein kinase
818 regulates FoxO1a and angiopoietin-2 in endothelial cells. *Cardiovasc Res*, 77, 160-8.
- 819 DUARTE, A., HIRASHIMA, M., BENEDITO, R., TRINDADE, A., DINIZ, P., BEKMAN, E.,
820 COSTA, L., HENRIQUE, D. & ROSSANT, J. 2004. Dosage-sensitive requirement for
821 mouse Dll4 in artery development. *Genes Dev*, 18, 2474-8.

- 822 DYER, M. A., FARRINGTON, S. M., MOHN, D., MUNDAY, J. R. & BARON, M. H. 2001.
823 Indian hedgehog activates hematopoiesis and vasculogenesis and can respecify
824 prospective neurectodermal cell fate in the mouse embryo. *Development*, 128, 1717-30.
- 825 DZIADEK, M. & ADAMSON, E. 1978. Localization and synthesis of alphafoetoprotein in post-
826 implantation mouse embryos. *J Embryol Exp Morphol*, 43, 289-313.
- 827 FANG, J. S., COON, B. G., GILLIS, N., CHEN, Z., QIU, J., CHITTENDEN, T. W., BURT, J.
828 M., SCHWARTZ, M. A. & HIRSCHI, K. K. 2017. Shear-induced Notch-Cx37-p27 axis
829 arrests endothelial cell cycle to enable arterial specification. *Nat Commun*, 8, 2149.
- 830 FERDOUS, A., MORRIS, J., ABEDIN, M. J., COLLINS, S., RICHARDSON, J. A. & HILL, J.
831 A. 2011. Forkhead factor FoxO1 is essential for placental morphogenesis in the
832 developing embryo. *Proc Natl Acad Sci U S A*, 108, 16307-12.
- 833 FISCHER, A., SCHUMACHER, N., MAIER, M., SENDTNER, M. & GESSLER, M. 2004. The
834 Notch target genes *Hey1* and *Hey2* are required for embryonic vascular development.
835 *Genes Dev*, 18, 901-11.
- 836 FISH, J. E., CANTU GUTIERREZ, M., DANG, L. T., KHYZHA, N., CHEN, Z., VEITCH, S.,
837 CHENG, H. S., KHOR, M., ANTOUNIANS, L., NJOCK, M. S., BOUDREAU, E.,
838 HERMAN, A. M., RHYNER, A. M., RUIZ, O. E., EISENHOFFER, G. T., MEDINA-
839 RIVERA, A., WILSON, M. D. & WYTHE, J. D. 2017. Dynamic regulation of VEGF-
840 inducible genes by an ERK/ERG/p300 transcriptional network. *Development*, 144, 2428-
841 2444.
- 842 FISH, J. E. & WYTHE, J. D. 2015. The molecular regulation of arteriovenous specification and
843 maintenance. *Dev Dyn*, 244, 391-409.
- 844 FOSBRINK, M., NICULESCU, F., RUS, V., SHIN, M. L. & RUS, H. 2006. C5b-9-induced
845 endothelial cell proliferation and migration are dependent on Akt inactivation of forkhead
846 transcription factor FOXO1. *J Biol Chem*, 281, 19009-18.
- 847 FRASER, S. T., HADJANTONAKIS, A. K., SAHR, K. E., WILLEY, S., KELLY, O. G.,
848 JONES, E. A., DICKINSON, M. E. & BARON, M. H. 2005. Using a histone yellow
849 fluorescent protein fusion for tagging and tracking endothelial cells in ES cells and mice.
850 *Genesis*, 42, 162-71.
- 851 FUKUMOTO, M., KONDO, K., UNI, K., ISHIGURO, T., HAYASHI, M., UEDA, S., MORI, I.,
852 NIIMI, K., TASHIRO, F., MIYAZAKI, S., MIYAZAKI, J. I., INAGAKI, S. &
853 FURUYAMA, T. 2018. Tip-cell behavior is regulated by transcription factor FoxO1
854 under hypoxic conditions in developing mouse retinas. *Angiogenesis*, 21, 203-214.
- 855 FURUYAMA, T., KITAYAMA, K., SHIMODA, Y., OGAWA, M., SONE, K., YOSHIDA-
856 ARAKI, K., HISATSUNE, H., NISHIKAWA, S., NAKAYAMA, K., NAKAYAMA, K.,
857 IKEDA, K., MOTOYAMA, N. & MORI, N. 2004. Abnormal angiogenesis in Foxo1
858 (*Fkhr*)-deficient mice. *J Biol Chem*, 279, 34741-9.
- 859 GALE, N. W., DOMINGUEZ, M. G., NOGUERA, I., PAN, L., HUGHES, V., VALENZUELA,
860 D. M., MURPHY, A. J., ADAMS, N. C., LIN, H. C., HOLASH, J., THURSTON, G. &
861 YANCOPOULOS, G. D. 2004. Haploinsufficiency of delta-like 4 ligand results in
862 embryonic lethality due to major defects in arterial and vascular development. *Proc Natl*
863 *Acad Sci U S A*, 101, 15949-54.
- 864 GOETZ, J. G., STEED, E., FERREIRA, R. R., ROTH, S., RAMSPACHER, C., BOSELLI, F.,
865 CHARVIN, G., LIEBLING, M., WYART, C., SCHWAB, Y. & VERMOT, J. 2014.
866 Endothelial cilia mediate low flow sensing during zebrafish vascular development. *Cell*
867 *Rep*, 6, 799-808.

- 868 GONG, Y., YANG, X., HE, Q., GOWER, L., PRUDOVSKY, I., VARY, C. P., BROOKS, P. C.
869 & FRIESEL, R. E. 2013. Sprouty4 regulates endothelial cell migration via modulating
870 integrin beta3 stability through c-Src. *Angiogenesis*, 16, 861-75.
- 871 GRIDLEY, T. 2010. Notch signaling in the vasculature. *Curr Top Dev Biol*, 92, 277-309.
- 872 HAYASHI, H. & KUME, T. 2008. Foxc transcription factors directly regulate Dll4 and Hey2
873 expression by interacting with the VEGF-Notch signaling pathways in endothelial cells.
874 *PLoS One*, 3, e2401.
- 875 HERMAN, A. M., RHYNER, A. M., DEVINE, W. P., MARRELLI, S. P., BRUNEAU, B. G. &
876 WYTHE, J. D. 2018. A novel reporter allele for monitoring Dll4 expression within the
877 embryonic and adult mouse. *Biol Open*, 7.
- 878 HERZOG, Y., GUTTMANN-RAVIV, N. & NEUFELD, G. 2005. Segregation of arterial and
879 venous markers in subpopulations of blood islands before vessel formation. *Dev Dyn*,
880 232, 1047-55.
- 881 HERZOG, Y., KALCHEIM, C., KAHANE, N., RESHEF, R. & NEUFELD, G. 2001.
882 Differential expression of neuropilin-1 and neuropilin-2 in arteries and veins. *Mech Dev*,
883 109, 115-9.
- 884 HOSAKA, T., BIGGS, W. H., 3RD, TIEU, D., BOYER, A. D., VARKI, N. M., CAVENEE, W.
885 K. & ARDEN, K. C. 2004. Disruption of forkhead transcription factor (FOXO) family
886 members in mice reveals their functional diversification. *Proc Natl Acad Sci U S A*, 101,
887 2975-80.
- 888 HUANG, H. & TINDALL, D. J. 2007. Dynamic FoxO transcription factors. *J Cell Sci*, 120,
889 2479-87.
- 890 HWA, J. J., BECKOUCHE, N., HUANG, L., KRAM, Y., LINDSKOG, H. & WANG, R. A.
891 2017. Abnormal arterial-venous fusions and fate specification in mouse embryos lacking
892 blood flow. *Sci Rep*, 7, 11965.
- 893 JI, R. P., PHOON, C. K., ARISTIZABAL, O., MCGRATH, K. E., PALIS, J. & TURNBULL, D.
894 H. 2003. Onset of cardiac function during early mouse embryogenesis coincides with
895 entry of primitive erythroblasts into the embryo proper. *Circ Res*, 92, 133-5.
- 896 JIANG, Z., TIAN, J., ZHANG, W., YAN, H., LIU, L., HUANG, Z., LOU, J. & MA, X. 2017.
897 Forkhead Protein FoxO1 Acts as a Repressor to Inhibit Cell Differentiation in Human
898 Fetal Pancreatic Progenitor Cells. *J Diabetes Res*, 2017, 6726901.
- 899 JIRAMONGKOL, Y. & LAM, E. W. 2020. FOXO transcription factor family in cancer and
900 metastasis. *Cancer Metastasis Rev*, 39, 681-709.
- 901 JONES, E. A., BARON, M. H., FRASER, S. E. & DICKINSON, M. E. 2004. Measuring
902 hemodynamic changes during mammalian development. *Am J Physiol Heart Circ*
903 *Physiol*, 287, H1561-9.
- 904 KAPPEL, A., RONICKE, V., DAMERT, A., FLAMME, I., RISAU, W. & BREIER, G. 1999.
905 Identification of vascular endothelial growth factor (VEGF) receptor-2 (Flk-1)
906 promoter/enhancer sequences sufficient for angioblast and endothelial cell-specific
907 transcription in transgenic mice. *Blood*, 93, 4284-92.
- 908 KIM, Y. H., CHOI, J., YANG, M. J., HONG, S. P., LEE, C. K., KUBOTA, Y., LIM, D. S. &
909 KOH, G. Y. 2019. A MST1-FOXO1 cascade establishes endothelial tip cell polarity and
910 facilitates sprouting angiogenesis. *Nat Commun*, 10, 838.
- 911 KISANUKI, Y. Y., HAMMER, R. E., MIYAZAKI, J., WILLIAMS, S. C., RICHARDSON, J.
912 A. & YANAGISAWA, M. 2001. Tie2-Cre transgenic mice: a new model for endothelial
913 cell-lineage analysis in vivo. *Dev Biol*, 230, 230-42.

- 914 KONDRYCHYN, I., KELLY, D. J., CARRETERO, N. T., NOMORI, A., KATO, K., CHONG,
915 J., NAKAJIMA, H., OKUDA, S., MOCHIZUKI, N. & PHNG, L. K. 2020. Marcks11
916 modulates endothelial cell mechanoresponse to haemodynamic forces to control blood
917 vessel shape and size. *Nat Commun*, 11, 5476.
- 918 KREBS, L. T., STARLING, C., CHERVONSKY, A. V. & GRIDLEY, T. 2010. Notch1
919 activation in mice causes arteriovenous malformations phenocopied by ephrinB2 and
920 EphB4 mutants. *Genesis*, 48, 146-50.
- 921 KREBS, L. T., XUE, Y., NORTON, C. R., SHUTTER, J. R., MAGUIRE, M., SUNDBERG, J.
922 P., GALLAHAN, D., CLOSSON, V., KITAJEWSKI, J., CALLAHAN, R., SMITH, G.
923 H., STARK, K. L. & GRIDLEY, T. 2000. Notch signaling is essential for vascular
924 morphogenesis in mice. *Genes Dev*, 14, 1343-52.
- 925 LAKSO, M., PICHEL, J. G., GORMAN, J. R., SAUER, B., OKAMOTO, Y., LEE, E., ALT, F.
926 W. & WESTPHAL, H. 1996. Efficient in vivo manipulation of mouse genomic
927 sequences at the zygote stage. *Proc Natl Acad Sci U S A*, 93, 5860-5.
- 928 LANGLET, F., HAEUSLER, R. A., LINDEN, D., ERICSON, E., NORRIS, T., JOHANSSON,
929 A., COOK, J. R., AIZAWA, K., WANG, L., BUETTNER, C. & ACCILI, D. 2017.
930 Selective Inhibition of FOXO1 Activator/Repressor Balance Modulates Hepatic Glucose
931 Handling. *Cell*, 171, 824-835 e18.
- 932 LAWSON, N. D., SCHEER, N., PHAM, V. N., KIM, C. H., CHITNIS, A. B., CAMPOS-
933 ORTEGA, J. A. & WEINSTEIN, B. M. 2001. Notch signaling is required for arterial-
934 venous differentiation during embryonic vascular development. *Development*, 128, 3675-
935 83.
- 936 LAWSON, N. D., VOGEL, A. M. & WEINSTEIN, B. M. 2002. sonic hedgehog and vascular
937 endothelial growth factor act upstream of the Notch pathway during arterial endothelial
938 differentiation. *Dev Cell*, 3, 127-36.
- 939 LE NOBLE, F., FLEURY, V., PRIES, A., CORVOL, P., EICHMANN, A. & RENEMAN, R. S.
940 2005. Control of arterial branching morphogenesis in embryogenesis: go with the flow.
941 *Cardiovasc Res*, 65, 619-28.
- 942 LE NOBLE, F., MOYON, D., PARDANAUD, L., YUAN, L., DJONOV, V., MATTHIJSSEN,
943 R., BREANT, C., FLEURY, V. & EICHMANN, A. 2004. Flow regulates arterial-venous
944 differentiation in the chick embryo yolk sac. *Development*, 131, 361-75.
- 945 LEE, S. H., SCHLOSS, D. J., JARVIS, L., KRASNOW, M. A. & SWAIN, J. L. 2001. Inhibition
946 of angiogenesis by a mouse sprouty protein. *J Biol Chem*, 276, 4128-33.
- 947 LIU, Z. J., SHIRAKAWA, T., LI, Y., SOMA, A., OKA, M., DOTTO, G. P., FAIRMAN, R. M.,
948 VELAZQUEZ, O. C. & HERLYN, M. 2003. Regulation of Notch1 and Dll4 by vascular
949 endothelial growth factor in arterial endothelial cells: implications for modulating
950 arteriogenesis and angiogenesis. *Mol Cell Biol*, 23, 14-25.
- 951 LOBOV, I. B., RENARD, R. A., PAPADOPOULOS, N., GALE, N. W., THURSTON, G.,
952 YANCOPOULOS, G. D. & WIEGAND, S. J. 2007. Delta-like ligand 4 (Dll4) is induced
953 by VEGF as a negative regulator of angiogenic sprouting. *Proc Natl Acad Sci U S A*, 104,
954 3219-24.
- 955 LUCITTI, J. L., JONES, E. A., HUANG, C., CHEN, J., FRASER, S. E. & DICKINSON, M. E.
956 2007. Vascular remodeling of the mouse yolk sac requires hemodynamic force.
957 *Development*, 134, 3317-26.
- 958 MACK, J. J. & IRUELA-ARISPE, M. L. 2018. NOTCH regulation of the endothelial cell
959 phenotype. *Curr Opin Hematol*, 25, 212-218.

- 960 MACK, J. J., MOSQUEIRO, T. S., ARCHER, B. J., JONES, W. M., SUNSHINE, H., FAAS, G.
961 C., BRIOT, A., ARAGON, R. L., SU, T., ROMAY, M. C., MCDONALD, A. I., KUO,
962 C. H., LIZAMA, C. O., LANE, T. F., ZOVEIN, A. C., FANG, Y., TARLING, E. J., DE
963 AGUIAR VALLIM, T. Q., NAVAB, M., FOGELMAN, A. M., BOUCHARD, L. S. &
964 IRUELA-ARISPE, M. L. 2017. NOTCH1 is a mechanosensor in adult arteries. *Nat*
965 *Commun*, 8, 1620.
- 966 MAILHOS, C., MODLICH, U., LEWIS, J., HARRIS, A., BICKNELL, R. & ISH-HOROWICZ,
967 D. 2001. Delta4, an endothelial specific notch ligand expressed at sites of physiological
968 and tumor angiogenesis. *Differentiation*, 69, 135-44.
- 969 MASUMURA, T., YAMAMOTO, K., SHIMIZU, N., OBI, S. & ANDO, J. 2009. Shear stress
970 increases expression of the arterial endothelial marker ephrinB2 in murine ES cells via
971 the VEGF-Notch signaling pathways. *Arterioscler Thromb Vasc Biol*, 29, 2125-31.
- 972 NIIMI, K., UEDA, M., FUKUMOTO, M., KOHARA, M., SAWANO, T., TSUCHIHASHI, R.,
973 SHIBATA, S., INAGAKI, S. & FURUYAMA, T. 2017. Transcription factor FOXO1
974 promotes cell migration toward exogenous ATP via controlling P2Y1 receptor expression
975 in lymphatic endothelial cells. *Biochem Biophys Res Commun*, 489, 413-419.
- 976 OBI, S., YAMAMOTO, K., SHIMIZU, N., KUMAGAYA, S., MASUMURA, T., SOKABE, T.,
977 ASAHARA, T. & ANDO, J. 2009. Fluid shear stress induces arterial differentiation of
978 endothelial progenitor cells. *J Appl Physiol (1985)*, 106, 203-11.
- 979 PAIK, J. H., KOLLIPARA, R., CHU, G., JI, H., XIAO, Y., DING, Z., MIAO, L., TOTHOVA,
980 Z., HORNER, J. W., CARRASCO, D. R., JIANG, S., GILLILAND, D. G., CHIN, L.,
981 WONG, W. H., CASTRILLON, D. H. & DEPINHO, R. A. 2007. FoxOs are lineage-
982 restricted redundant tumor suppressors and regulate endothelial cell homeostasis. *Cell*,
983 128, 309-23.
- 984 PALIS, J. 2014. Primitive and definitive erythropoiesis in mammals. *Front Physiol*, 5, 3.
- 985 PFAFFL, M. W. 2001. A new mathematical model for relative quantification in real-time RT-
986 PCR. *Nucleic Acids Res*, 29, e45.
- 987 POTENTE, M., URBICH, C., SASAKI, K., HOFMANN, W. K., HEESCHEN, C., AICHER, A.,
988 KOLLIPARA, R., DEPINHO, R. A., ZEIHNER, A. M. & DIMMELER, S. 2005.
989 Involvement of Foxo transcription factors in angiogenesis and postnatal
990 neovascularization. *J Clin Invest*, 115, 2382-92.
- 991 RIDDELL, M., NAKAYAMA, A., HIKITA, T., MIRZAPOURSHAFIYI, F., KAWAMURA, T.,
992 PASHA, A., LI, M., MASUZAWA, M., LOOSO, M., STEINBACHER, T., EBNET, K.,
993 POTENTE, M., HIROSE, T., OHNO, S., FLEMING, I., GATTENLOHNER, S., AUNG,
994 P. P., PHUNG, T., YAMASAKI, O., YANAGI, T., UMEMURA, H. & NAKAYAMA,
995 M. 2018. aPKC controls endothelial growth by modulating c-Myc via FoxO1 DNA-
996 binding ability. *Nat Commun*, 9, 5357.
- 997 RISAU, W. 1994. Angiogenesis and endothelial cell function. *Arzneimittelforschung*, 44, 416-7.
- 998 RISAU, W. & FLAMME, I. 1995. Vasculogenesis. *Annu Rev Cell Dev Biol*, 11, 73-91.
- 999 RONICKE, V., RISAU, W. & BREIER, G. 1996. Characterization of the endothelium-specific
1000 murine vascular endothelial growth factor receptor-2 (Flk-1) promoter. *Circ Res*, 79, 277-
1001 85.
- 1002 RUDNICKI, M., ABDIFARKOSH, G., NWADOZI, E., RAMOS, S. V., MAKKI, A., SEPA-
1003 KISHI, D. M., CEDDIA, R. B., PERRY, C. G., ROUDIER, E. & HAAS, T. L. 2018.
1004 Endothelial-specific FoxO1 depletion prevents obesity-related disorders by increasing
1005 vascular metabolism and growth. *Elife*, 7.

- 1006 SACILOTTO, N., MONTEIRO, R., FRITZSCHE, M., BECKER, P. W., SANCHEZ-DEL-
1007 CAMPO, L., LIU, K., PINHEIRO, P., RATNAYAKA, I., DAVIES, B., GODING, C. R.,
1008 PATIENT, R., BOU-GHARIOS, G. & DE VAL, S. 2013. Analysis of Dll4 regulation
1009 reveals a combinatorial role for Sox and Notch in arterial development. *Proc Natl Acad*
1010 *Sci U S A*, 110, 11893-8.
- 1011 SENGUPTA, A., CHAKRABORTY, S., PAIK, J., YUTZEY, K. E. & EVANS-ANDERSON,
1012 H. J. 2012. FoxO1 is required in endothelial but not myocardial cell lineages during
1013 cardiovascular development. *Dev Dyn*, 241, 803-13.
- 1014 SEO, S., FUJITA, H., NAKANO, A., KANG, M., DUARTE, A. & KUME, T. 2006. The
1015 forkhead transcription factors, Foxc1 and Foxc2, are required for arterial specification
1016 and lymphatic sprouting during vascular development. *Dev Biol*, 294, 458-70.
- 1017 SHAY-SALIT, A., SHUSHY, M., WOLFOVITZ, E., YAHAV, H., BREVIARIO, F., DEJANA,
1018 E. & RESNICK, N. 2002. VEGF receptor 2 and the adherens junction as a mechanical
1019 transducer in vascular endothelial cells. *Proc Natl Acad Sci U S A*, 99, 9462-7.
- 1020 SHUTTER, J. R., SCULLY, S., FAN, W., RICHARDS, W. G., KITAJEWSKI, J.,
1021 DEBLANDRE, G. A., KINTNER, C. R. & STARK, K. L. 2000. Dll4, a novel Notch
1022 ligand expressed in arterial endothelium. *Genes Dev*, 14, 1313-8.
- 1023 SIEKMANN, A. F. & LAWSON, N. D. 2007. Notch signalling limits angiogenic cell behaviour
1024 in developing zebrafish arteries. *Nature*, 445, 781-4.
- 1025 SU, T., STANLEY, G., SINHA, R., D'AMATO, G., DAS, S., RHEE, S., CHANG, A. H.,
1026 PODURI, A., RAFTREY, B., DINH, T. T., ROPER, W. A., LI, G., QUINN, K. E.,
1027 CARON, K. M., WU, S., MIQUEROL, L., BUTCHER, E. C., WEISSMAN, I., QUAKE,
1028 S. & RED-HORSE, K. 2018. Single-cell analysis of early progenitor cells that build
1029 coronary arteries. *Nature*, 559, 356-362.
- 1030 SUN, X., CHEN, W. D. & WANG, Y. D. 2017. DAF-16/FOXO Transcription Factor in Aging
1031 and Longevity. *Front Pharmacol*, 8, 548.
- 1032 SWIFT, M. R. & WEINSTEIN, B. M. 2009. Arterial-venous specification during development.
1033 *Circ Res*, 104, 576-88.
- 1034 TANIGUCHI, K., ISHIZAKI, T., AYADA, T., SUGIYAMA, Y., WAKABAYASHI, Y.,
1035 SEKIYA, T., NAKAGAWA, R. & YOSHIMURA, A. 2009. Sprouty4 deficiency
1036 potentiates Ras-independent angiogenic signals and tumor growth. *Cancer Sci*, 100,
1037 1648-54.
- 1038 TZIMA, E., IRANI-TEHRANI, M., KIOSSES, W. B., DEJANA, E., SCHULTZ, D. A.,
1039 ENGELHARDT, B., CAO, G., DELISSER, H. & SCHWARTZ, M. A. 2005. A
1040 mechanosensory complex that mediates the endothelial cell response to fluid shear stress.
1041 *Nature*, 437, 426-31.
- 1042 UDAN, R. S., VADAKKAN, T. J. & DICKINSON, M. E. 2013. Dynamic responses of
1043 endothelial cells to changes in blood flow during vascular remodeling of the mouse yolk
1044 sac. *Development*, 140, 4041-50.
- 1045 WANG, H. U., CHEN, Z. F. & ANDERSON, D. J. 1998. Molecular distinction and angiogenic
1046 interaction between embryonic arteries and veins revealed by ephrin-B2 and its receptor
1047 Eph-B4. *Cell*, 93, 741-53.
- 1048 WEINSTEIN, B. M. & LAWSON, N. D. 2002. Arteries, veins, Notch, and VEGF. *Cold Spring*
1049 *Harb Symp Quant Biol*, 67, 155-62.

- 1050 WIETecha, M. S., CHEN, L., RANZER, M. J., ANDERSON, K., YING, C., PATEL, T. B. &
1051 DIPIETRO, L. A. 2011. Sprouty2 downregulates angiogenesis during mouse skin wound
1052 healing. *Am J Physiol Heart Circ Physiol*, 300, H459-67.
- 1053 WILHELM, K., HAPPEL, K., EELEN, G., SCHOORS, S., OELLERICH, M. F., LIM, R.,
1054 ZIMMERMANN, B., ASPALTER, I. M., FRANCO, C. A., BOETTGER, T., BRAUN,
1055 T., FRUTTIGER, M., RAJEWSKY, K., KELLER, C., BRUNING, J. C., GERHARDT,
1056 H., CARMELIET, P. & POTENTE, M. 2016. FOXO1 couples metabolic activity and
1057 growth state in the vascular endothelium. *Nature*, 529, 216-20.
- 1058 WRAGG, J. W., DURANT, S., MCGETTRICK, H. M., SAMPLE, K. M., EGGINTON, S. &
1059 BICKNELL, R. 2014. Shear stress regulated gene expression and angiogenesis in
1060 vascular endothelium. *Microcirculation*, 21, 290-300.
- 1061 WYTHE, J. D., DANG, L. T., DEVINE, W. P., BOUDREAU, E., ARTAP, S. T., HE, D.,
1062 SCHACHTERLE, W., STAINIER, D. Y., OETTGEN, P., BLACK, B. L., BRUNEAU,
1063 B. G. & FISH, J. E. 2013. ETS factors regulate Vegf-dependent arterial specification.
1064 *Dev Cell*, 26, 45-58.
- 1065 XUE, Y., GAO, X., LINDSELL, C. E., NORTON, C. R., CHANG, B., HICKS, C., GENDRON-
1066 MAGUIRE, M., RAND, E. B., WEINMASTER, G. & GRIDLEY, T. 1999. Embryonic
1067 lethality and vascular defects in mice lacking the Notch ligand Jagged1. *Hum Mol Genet*,
1068 8, 723-30.
- 1069 YOU, L. R., LIN, F. J., LEE, C. T., DEMAYO, F. J., TSAI, M. J. & TSAI, S. Y. 2005.
1070 Suppression of Notch signalling by the COUP-TFII transcription factor regulates vein
1071 identity. *Nature*, 435, 98-104.
- 1072 ZHANG, H., GE, S., HE, K., ZHAO, X., WU, Y., SHAO, Y. & WU, X. 2019. FoxO1 inhibits
1073 autophagosome-lysosome fusion leading to endothelial autophagic-apoptosis in diabetes.
1074 *Cardiovasc Res*, 115, 2008-2020.
- 1075 ZHAO, Y., YANG, J., LIAO, W., LIU, X., ZHANG, H., WANG, S., WANG, D., FENG, J., YU,
1076 L. & ZHU, W. G. 2010. Cytosolic FoxO1 is essential for the induction of autophagy and
1077 tumour suppressor activity. *Nat Cell Biol*, 12, 665-75.
- 1078

Fig. 1

bioRxiv preprint doi: <https://doi.org/10.1101/2021.09.02.458792>; this version posted September 4, 2021. The copyright holder for this preprint (which was not certified by peer review) is the author/funder. All rights reserved. No reuse allowed without permission.

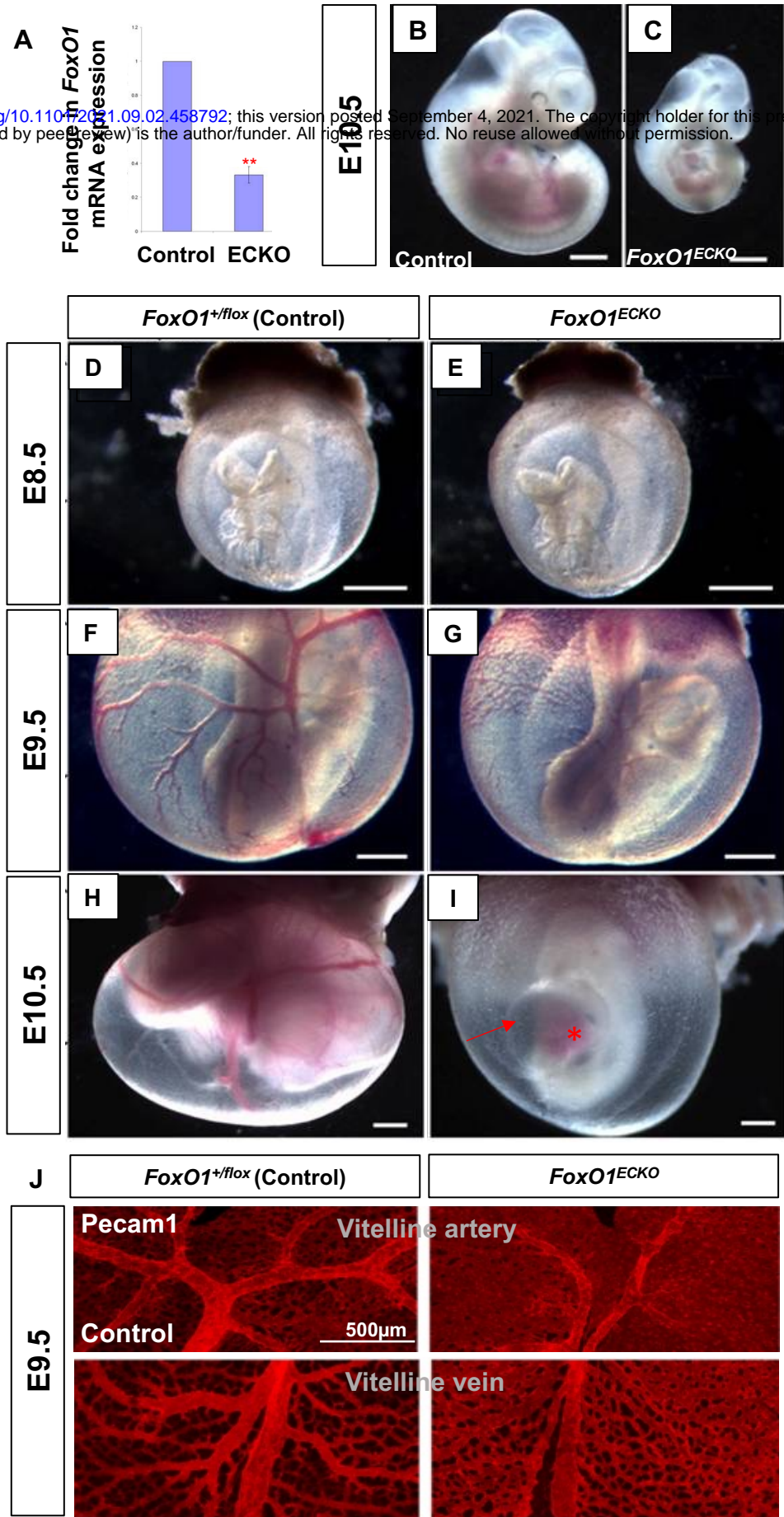


Fig. 2

bioRxiv preprint doi: <https://doi.org/10.1101/2020.09.02.458792>; this version posted September 4, 2021. The copyright holder for this preprint (which was not certified by peer review) is the author/funder. All rights reserved. No reuse allowed without permission.

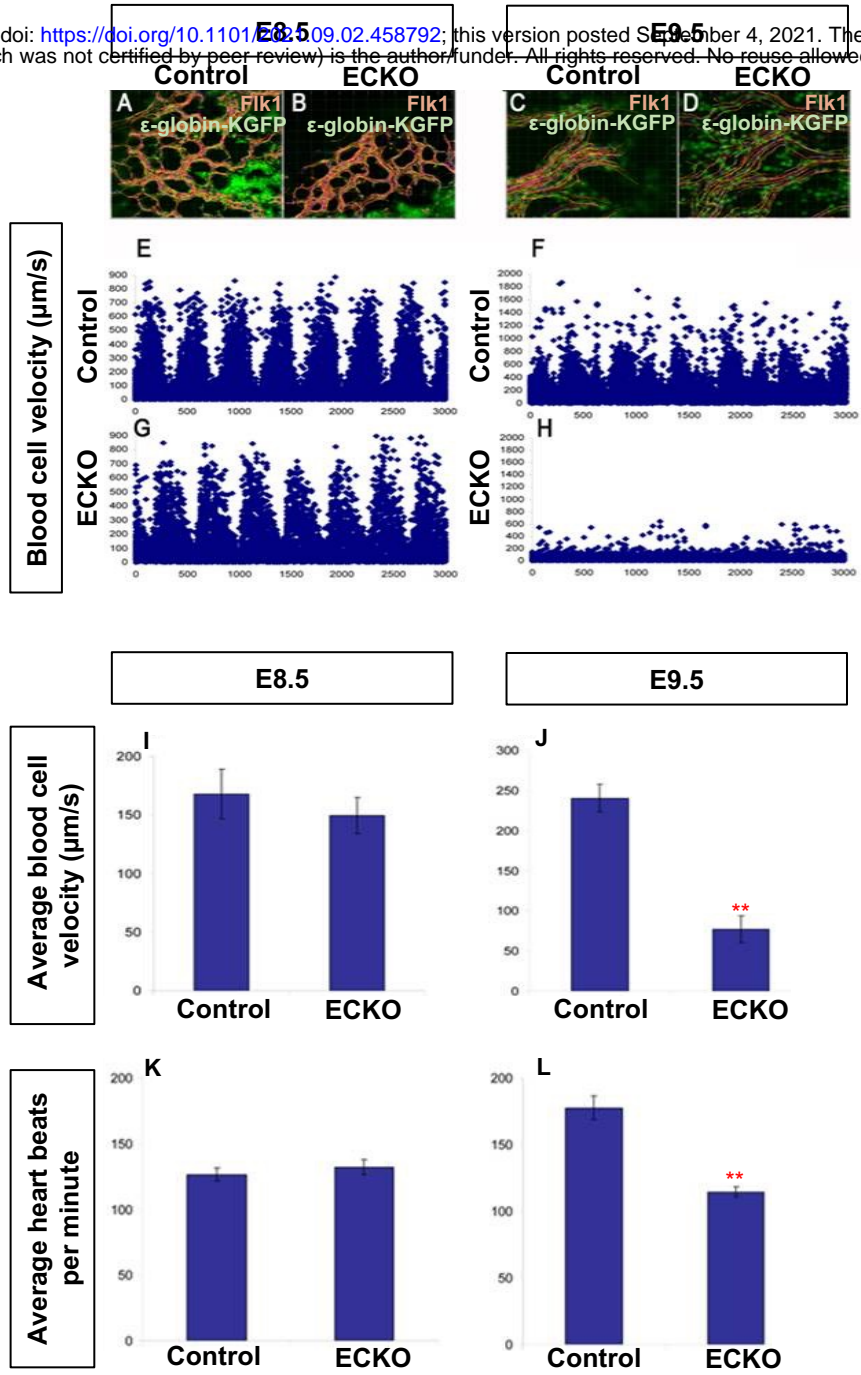


Table 1

	Genotype	Number	Percent of Total	Gross Allantois Defects	Percent of genotype
4 Litters	WT	16	31.37		
	<i>FoxO1^{floxdel/+}</i>	20	39.21		
	<i>FoxO1^{floxdel/floxdel}</i>	15	29.41	2	13.33
	Total	51			
6 Litters	<i>FoxO1^{flox/+}</i>	15	31.91		
	<i>FoxO1^{flox/+};Tie2-cre^{Tg/+}</i>	12	25.53		
	<i>FoxO1^{flox/flox}</i>	10	21.27		
	<i>FoxO1^{flox/flox};Tie2-cre^{Tg/+}</i>	10	21.27	0	0
	Total	47			

Fig. 3

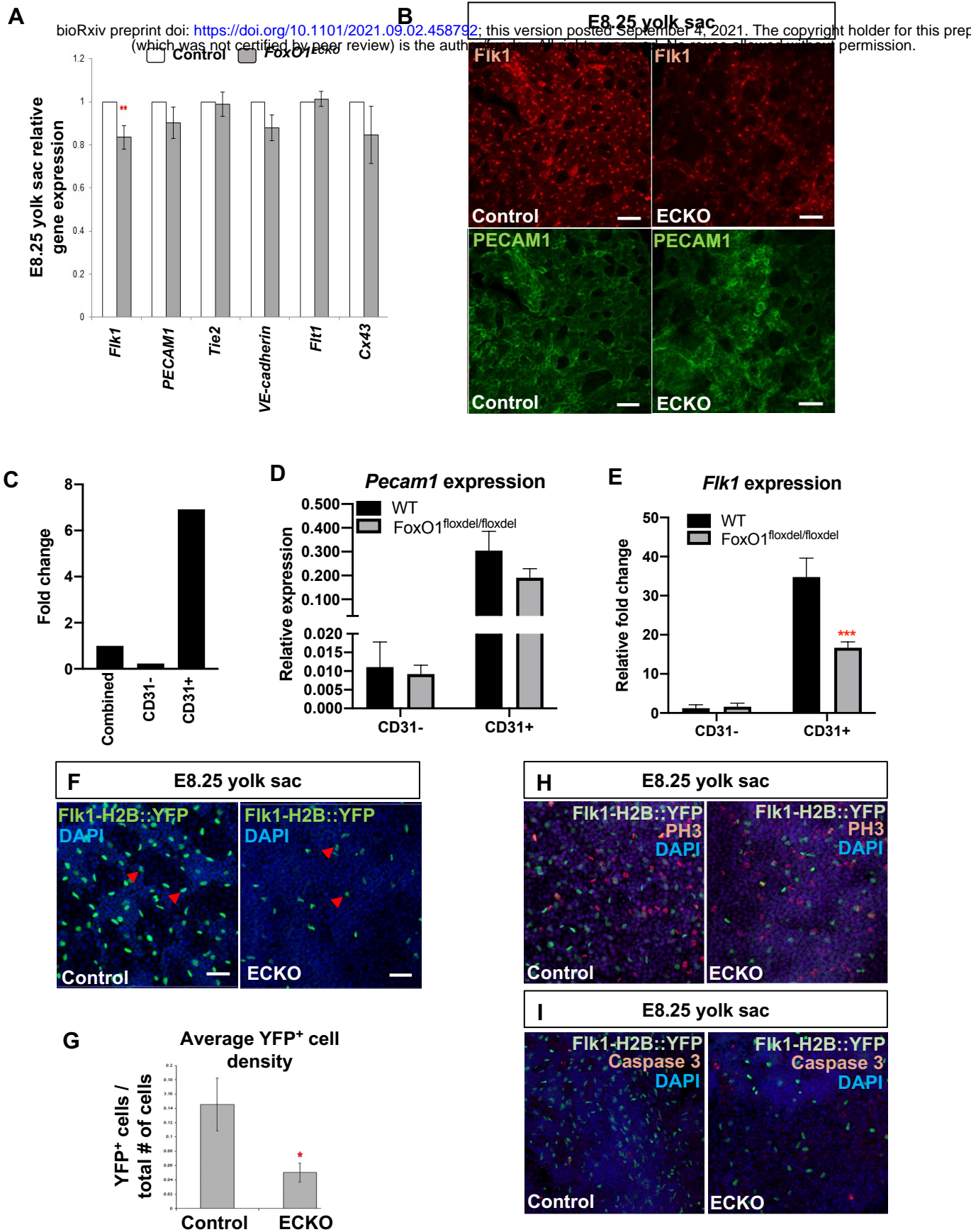


Fig. 4

bioRxiv preprint doi: <https://doi.org/10.1101/2021.09.02.458792>; this version posted September 4, 2021. The copyright holder for this preprint (which was not certified by peer review) is the author/funder. All rights reserved. No reuse allowed without permission.

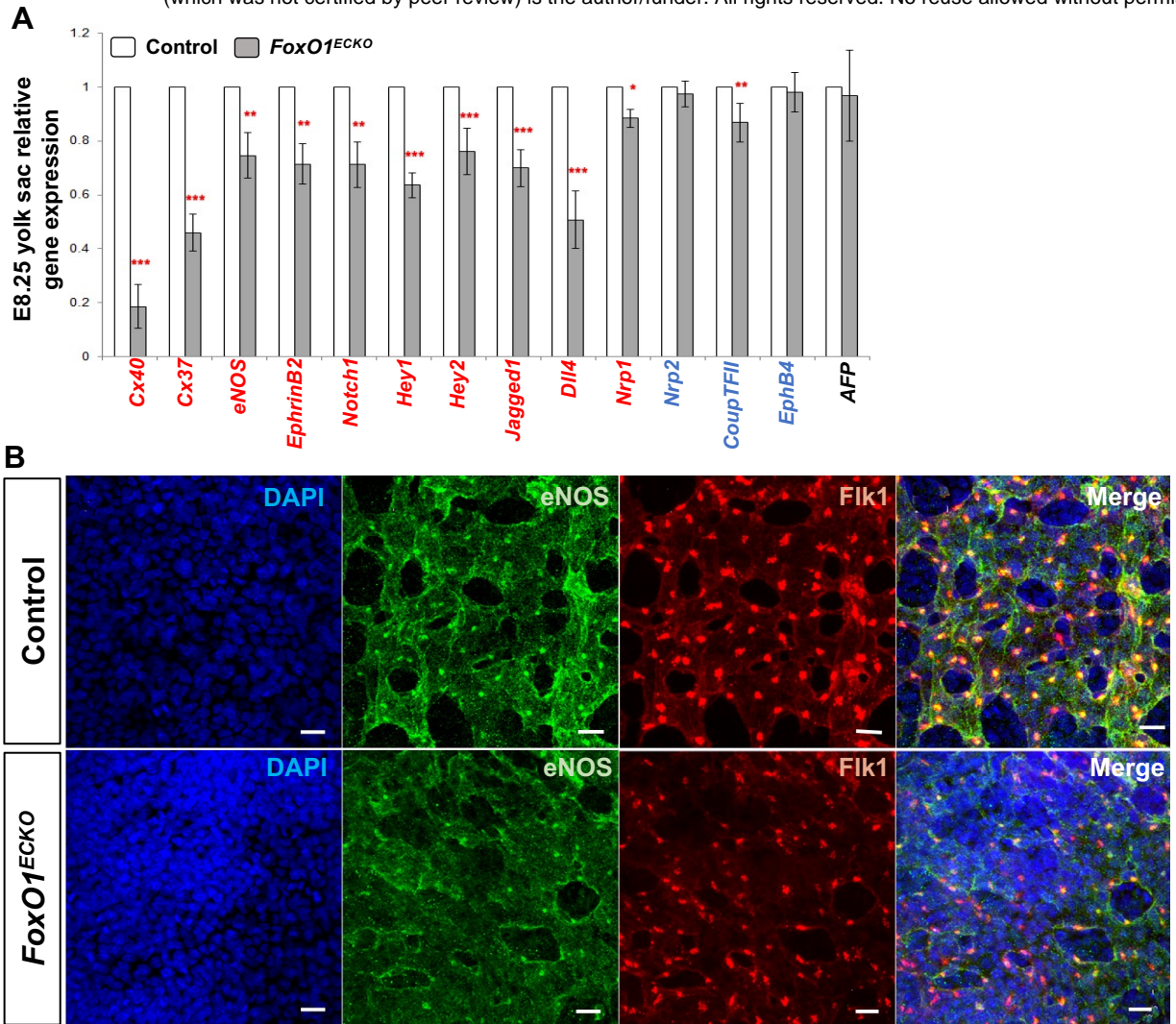


Fig. 5

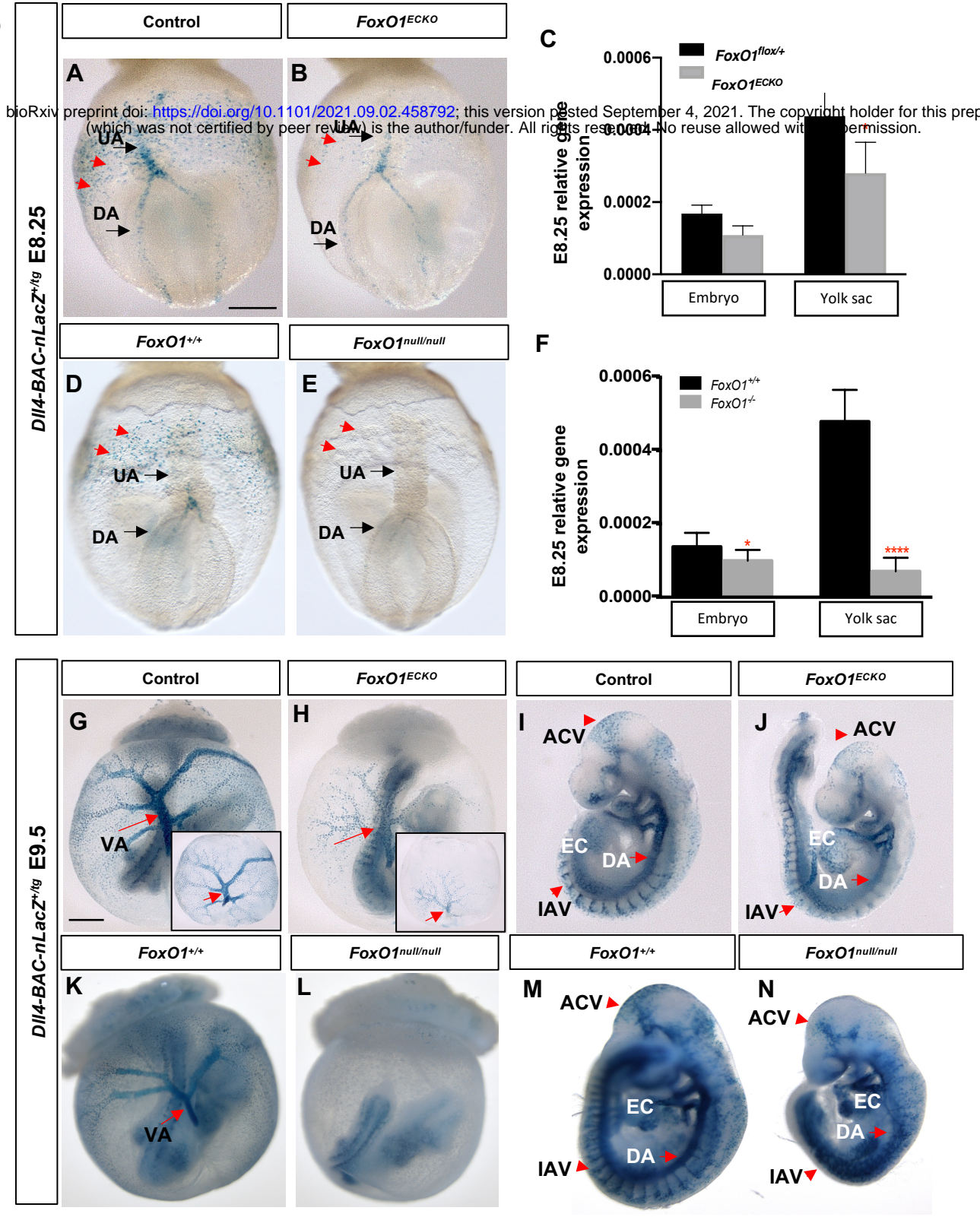


Fig. 6

bioRxiv preprint doi: <https://doi.org/10.1101/2021.09.02.458792>; this version posted September 4, 2021. The copyright holder for this preprint (which was not certified by peer review) is the author/funder. All rights reserved. No reuse allowed without permission.

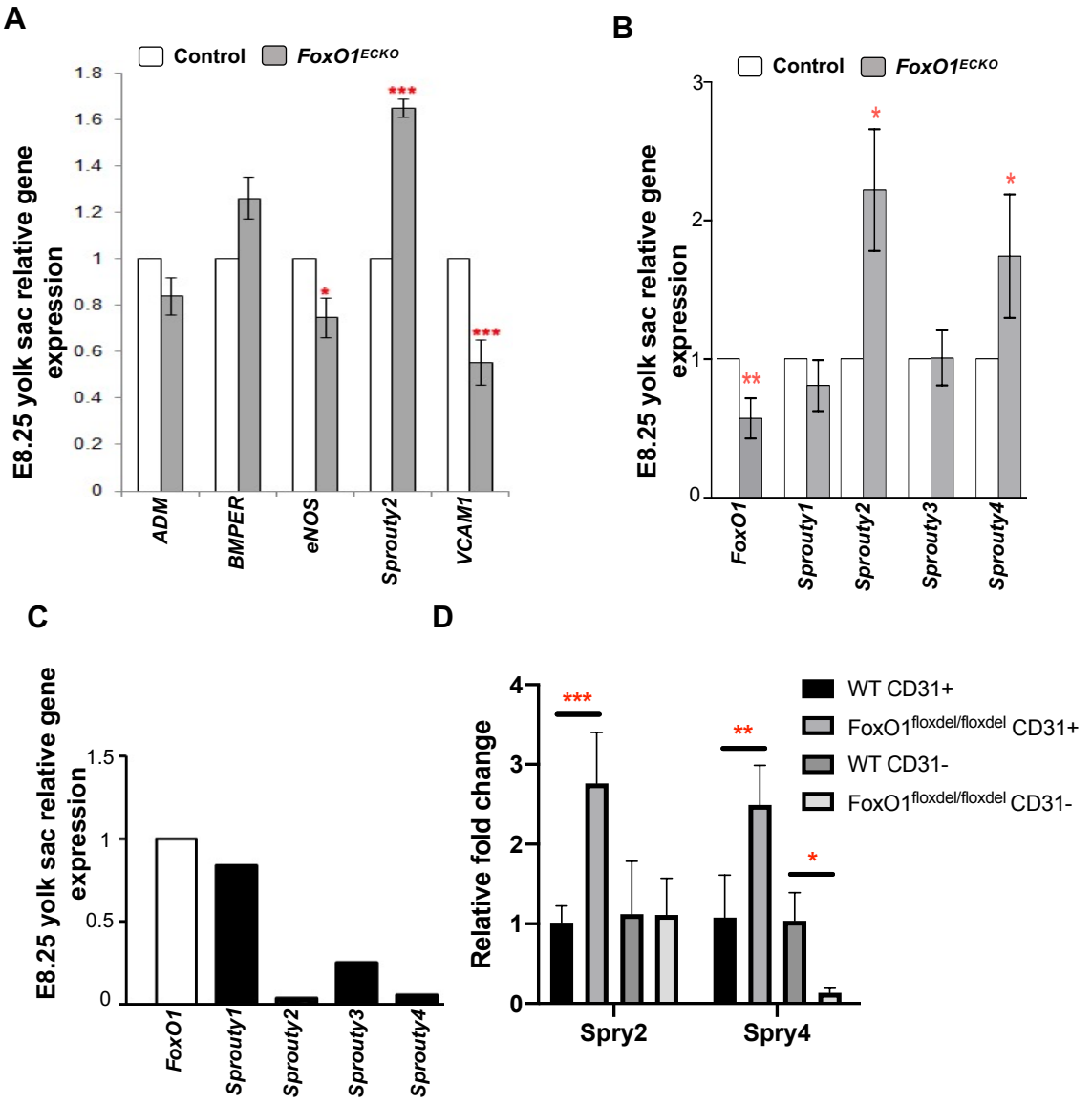


Fig. 7

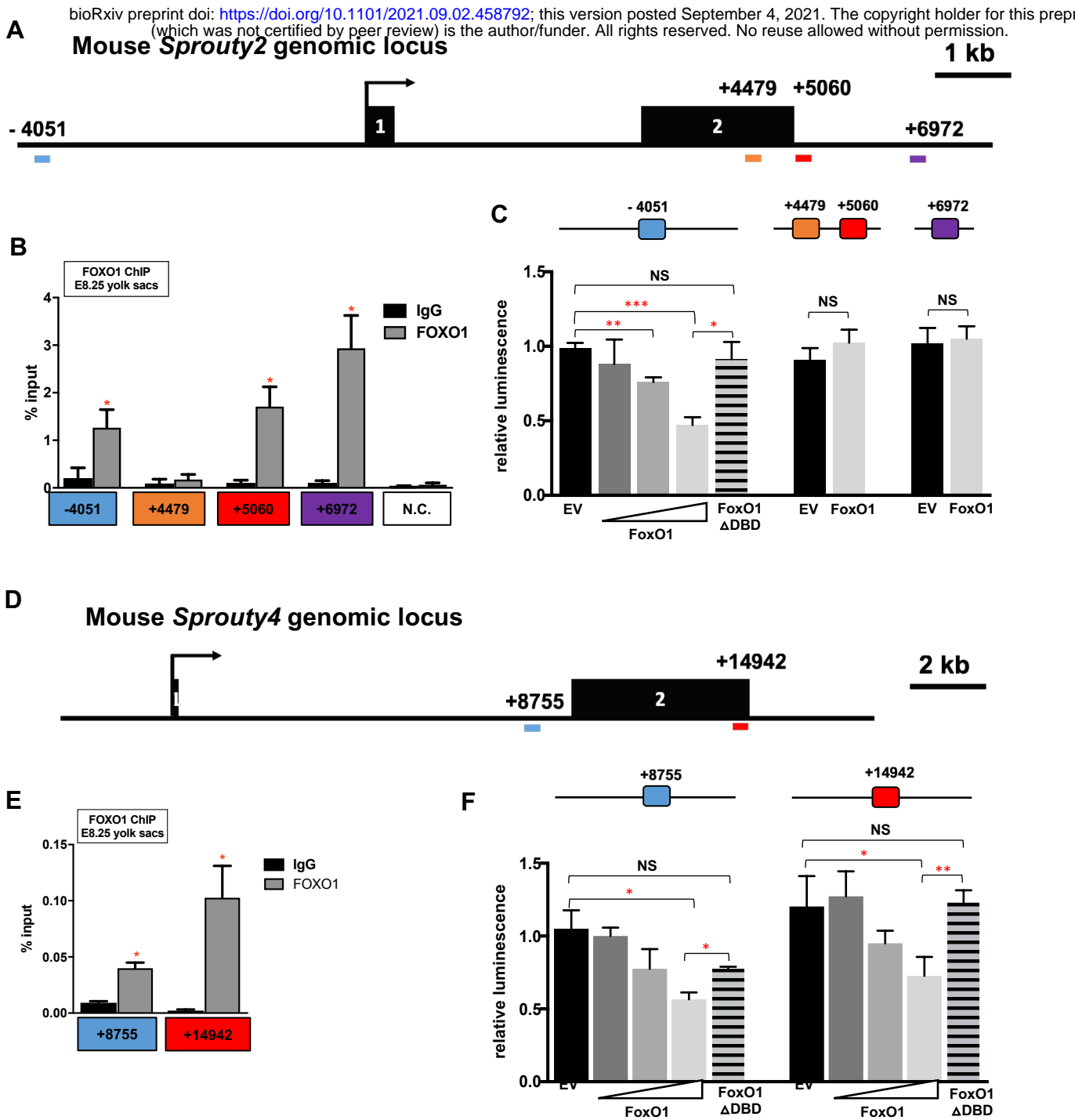


Fig. 8

bioRxiv preprint doi: <https://doi.org/10.1101/2021.09.02.458792>; this version posted September 4, 2021. The copyright holder for this preprint (which was not certified by peer review) is the author/funder. All rights reserved. No reuse allowed without permission.

